

## ABSTRACT

Title of Thesis: IDENTIFICATION OF PRECURSER SIGNALS TO  
IMPENDING COOKING RELATED FIRES

Robin E. Zevotek, Fire Protection Engineering, and 2015

Thesis directed By: Professor and Chair, Dr. Jim A. Milke, Department of  
Fire Protection Engineering

Cooking related fires continue to be the leading cause of fires in homes. In an effort to reduce the number of cooking fires Underwriters Laboratories (UL) and the University of Maryland (UMD) partnered to evaluate detection of cooking related fires. An experimental protocol was developed to examine if precursor signals capable of predicting an impending fire can be detected to provide adequate warning prior to flaming fire. A series of eleven different experiments were conducted to acquire signals from sensors located at or near an electric coil range. The data recorded was analyzed to identify element gas temperature, carbon monoxide concentration, optical density and ionization signal as potential indicators of an impending fire. Further work is needed to evaluate sensor threshold values and the algorithms developed for other cooking styles and cooking appliances.

IDENTIFICATION OF PRECURSER SIGNALS TO IMPENDING COOKING  
RELATED FIRES

By

Robin E. Zevotek

Thesis submitted to the Faculty of the Graduate School of the  
University of Maryland, College Park, in partial fulfillment  
of the requirements for the degree of  
Masters of Science  
2015

Advisory Committee:  
Dr. James Milke, Chair  
Dr. Thomas Fabian  
Dr. Stanislav Stoliarov

©Copyright by  
Robin E. Zevotek  
2015

## Preface

Cooking related equipment fires continue to be the leading cause of fires in homes. In an effort to reduce the number of cooking fires Underwriters Laboratories (UL) and the University of Maryland (UMD) partnered to evaluate detection of cooking related fires. An experimental protocol was developed to examine if precursor signals capable of predicting an impending fire can be detected to provide adequate warning to homeowners in order to intervene and prevent transition to flaming fire.

A series of eleven different cooking scenarios were conducted in a full scale kitchen mockup within a two story house built in the large fire laboratory at UL. Scenarios were selected to demonstrate a range of cooking styles and types with varying dishes including cooking with grease and oils where the potential for a flaming fire exists. The kitchen was outfitted with optical density meters, temperature sensors, heat flux gauges, gas sensors, and smoke alarms. Data was recorded in close proximity to the cooking range along with various points within the kitchen space. High definition video was collected along with thermal imaging to provide visual information about the conditions within the space. The recorded data was then provided to the UMD for organization and analysis.

UMD was tasked with organizing and evaluating the data collected by UL for precursor signals which indicate an impending fire scenario. The data was organized based on hazard potential in order to develop normal cooking and potential impending fire categories. Each sensor was then evaluated to determine patterns associated with impending fires. From this analysis it was found

that element gas temperature, carbon monoxide concentration, optical density and ionization signal all provided some indication of an impending fire.

In order to develop the most effective and reliable precursor, the response of the sensors was evaluated using two algorithms to identify the most suitable approach for distinguishing an impending cooking fire from normal cooking while providing sufficient notice for preventative intervention. The combination of element gas temperature and optical density demonstrated the ability to detect all of the impending cooking fires and hazardous conditions tested with no false positives. The sensor provided adequate response time in all but one experiment which did not represent a cooking hazard but the ignition of a material left on a hot burner.

Further work is needed to evaluate the sensor threshold values and algorithms developed for more other cooking styles and conditions; however, it appears that precursor signals to impending cooking related fires can be developed through both individual sensors and a combination of individual sensors and advanced algorithm.

## Acknowledgements

I would like to acknowledge the opportunity and support received on this work from Underwriters Laboratories (UL), specifically Dr. Thomas Fabian. Dr Fabian provided immense support in understanding the complexity of the testing and instrumentation involved in the experiments along with continuous advisement. It was a privilege to learn and grow as an engineer with his support.

In addition to Dr. Fabian, Director of UL's Firefighter Safety Research Institute Steve Kerber provided additional support and mentorship through the work. This work would not have been possible without Mr. Kerber's support.

I would also like to thank Dr. Jim Milke, P.E. Professor and Chair with the Department of Fire Protection Engineering at the University of Maryland. Dr. Milke has served as a professor and mentor though out my undergraduate and graduate terms at the University of Maryland. It has been an honor to work under and learn from such a dedicated professor and fire protection engineer who illustrates such an unprecedented drive for the advancement of fire protection engineering. Without his patience, understanding, knowledge and support this work would not have been possible.

Finally I'd like to thank my supportive, understanding, patient, caring and all around wonderful fiancé Christina Bryz-Gornia for help through the process of conducting this work.

# Table of Contents

Chapter 1: Background .....	10
Chapter 2: Previous Work.....	15
Chapter 3: Experimental Setup .....	21
3.1 Kitchen Setup.....	21
3.2 Range Setup .....	23
3.3 Sensor Setup/Location .....	23
3.4 Video.....	28
3.5 Limitations .....	29
Pan Mass & Material .....	29
Kitchen Ventilation.....	29
Range Heat Source.....	30
Sensor Location .....	30
3.7 Experiments .....	30
Chapter 4: Data: Initial Analysis.....	38
4.1 Identification of Stages (Normal, Pre-Fire/Action, Fire).....	38
4.2 Sensor Results.....	42
Chapter 5: Analysis: Algorithm Development .....	74
5.1 Individual Sensor Algorithms .....	74
5.2 Multi-Sensor Algorithms .....	88
Chapter 6: Summary .....	94
Chapter 7: Future Work .....	96
7.1 Other Cooking Styles.....	96
7.2 Additional Potential Precursor Signals .....	97
References.....	99

## List of Tables

Table 1: Pan Thermal Inertia Data (Consumer Product Safety Commission, 1998).....	16
Table 1: Cooking Fire Experiments.....	31
Table 2: Normal Cooking Data Criteria.....	39
Table 4: Centerline Pan Temperatures Minimum and Maximum for Normal and Pre-Fire – All Experiments .....	42
Table 5: Kitchen Thermocouple Array values Normal and Pre-Fire – All Experiments .....	43
Table 6: Pan Temperature Normal and Pre-Fire – All Experiments .....	44
Table 7: Element Temperature Normal & Pre-Fire – All experiments .....	48
Table 8: Average Particle Size Normal & Pre-Fire – All Experiments.....	51
Table 9: Maximum Particle Density Normal & Pre-Fire – All Experiments .....	52
Table 10: Maximum CO <sub>2</sub> ppm Normal Cooking & Pre-Fire – All Experiments .....	56
Table 11: Maximum CO ppm Normal Cooking & Pre-Fire – All Experiments .....	58
Table 12: Maximum Obscuration during Normal Cooking & Pre-Fire – All Experiments .....	61
Table 13: Maximum Heat Flux for Normal and Pre-Fire Stage – All Experiments.....	64
Table 14: Range Analog Alarm Normal Cooking and Pre-Fire Stage – All Experiments .....	65
Table 15: Kitchen Analog Alarm Normal Cooking and Pre-Fire Stage – All Experiments.....	66
Table 16: Range and Kitchen Analog CO Alarm Normal Cooking and Pre-Fire Stage – All Experiments .....	67
Table 17: Commercially Available Ion/CO alarm Analog Signal Normal Cooking and Pre-Fire – All Experiments .....	68
Table 18: Advanced Algorithm Ion Alarm Response Time .....	73
Table 19: Element Temperature Algorithm Response Time .....	76
Table 20: CO Algorithm Response Time .....	79
Table 21: Optical Density Algorithm Response Time.....	82
Table 22: Ionization Signal Algorithm .....	86
Table 23: Sensor Performance Comparison – Single Sensor vs. Multi Sensor .....	90



## List of Figures

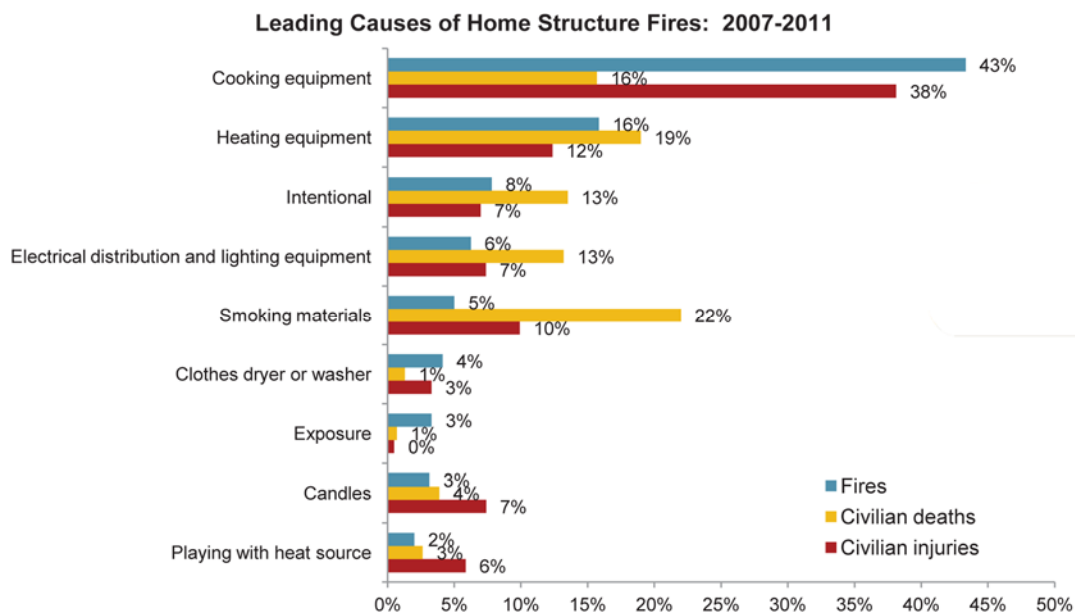
Figure 1: Leading Causes of Home Structure Fires 2007-2011 (Ahrens, 2013) .....	10
Figure 2: U.S. Fire Incident Trends (in Thousands) 1997-2011 (Levesque, 2013).....	11
Figure 3: Cooking Related Fires (in Thousands) 1980-2010 (Aherns, 2012) .....	12
Figure 4: Kitchen Layout.....	22
Figure 5: Pan Thermocouple Position.....	23
Figure 6: Range Sensor Setup.....	25
Figure 7: Element Thermocouple .....	25
Figure 8: Kitchen Smoke Alarm Array.....	28
Figure 9: Experiment 1 – Chronological Images.....	23
Figure 10: Experiment 1 – Ground Beef Result .....	23
Figure 11: Experiment 2 – Chronological Images.....	24
Figure 12: Experiment 2 – Ground Beef Result .....	24
Figure 13: Experiment 3 – Chronological Images.....	26
Figure 14: Experiment 3 – Blackened Fish Result .....	26
Figure 15: Experiment 4 – Chronological Images.....	28
Figure 16: Experiment 4 – Vegetables Result .....	28
Figure 17: Experiment 5 – Chronological Images.....	29
Figure 18: Experiment 5 – Seared Steak Result .....	30
Figure 19: Experiment 6 – Chronological Images.....	31
Figure 20: Experiment 7 – Chronological Images.....	32
Figure 21: Experiment 7 – Bacon Start.....	33
Figure 22: Experiment 8 – Chronological Images.....	34
Figure 23: Experiment 9 – Chronological Images.....	34
Figure 24: Experiment 10 – Pan & French Fries Setup .....	35
Figure 25: Experiment 10 – Chronological Images.....	36
Figure 26: Experiment 11 - Chronological Images.....	37
Figure 27: Anderson-Darling Probability Plot – CPSC Thermal Inertia Data .....	41
Figure 28: Time to Maximum Temperature Histogram & Normal Fit for CPSC Thermal Inertia Data.....	41
Figure 29: Pan Temperature Range – Normal Cooking and Pre-Fire .....	45
Figure 30: Experiment 6 Pan & Element Temperature Graph .....	46
Figure 31: Experiment 3 Pan and Element Temperature Graph.....	47
Figure 32: Element Temperature Range – Normal Cooking and Pre-Fire .....	48
Figure 33: Experiment 6 – Particle Size Distribution.....	50
Figure 34: Particle Density Range – Normal Cooking and Pre-Fire .....	53
Figure 35: Oxygen Concentration – All Experiments .....	55
Figure 36: Comparison CO <sub>2</sub> Percentage Concentration to CO <sub>2</sub> ppm for all experiments .....	56
Figure 37: Carbon Monoxide Concentration Range – Normal Cooking and Pre-Fire .....	58
Figure 38: Partial CO ppm Experiment 9 – Corn Oil .....	59
Figure 39: Smoke Obscuration per Meter above Range – Experiment 6 – Corn Oil .....	60
Figure 40: Experiment 10 – Optical Density above Range .....	62
Figure 41: Optical Density Range – Normal Cooking and Pre-Fire.....	62
Figure 42: Experiment 11 – Optical Density above Range .....	63

Figure 43: Range of Alarm Signal from Ionization Alarm located on Ceiling above Pan – Normal and Pre-Fire Stages .....	65
Figure 44: Commercially Available Ion/CO Alarm Response.....	69
Figure 45: Ionization vs. Photoelectric Alarm Response.....	70
Figure 46: Combination Photo/Ion Alarm Response.....	71
Figure 47: Photoelectric and Photo/CO Alarm Comparison .....	72
Figure 48: Advanced Algorithm Ion Alarm Response Graph .....	73
Figure 49: Histogram of Element Temperature Distribution during Normal & Pre-Fire.....	75
Figure 50: Element Temperature Algorithm Response .....	76
Figure 51: Element Temperature Threshold Analysis.....	77
Figure 52: CO ppm Data Distribution Normal& Pre-Fire .....	78
Figure 53: CO Algorithm Response .....	79
Figure 54: CO ppm Multi Threshold Analysis .....	80
Figure 55: Optical Density Data Distribution Normal & Pre-Fire .....	81
Figure 56: Optical Density Algorithm Response.....	82
Figure 57: Optical Density Threshold Analysis.....	83
Figure 58: Ionization Signal Activation Data Probability Plot.....	84
Figure 59: Ionization Signal Activation Data Distribution.....	84
Figure 60: Probability Plot of Ionization Signal – Normal Cooking Data .....	85
Figure 61: Ionization Signal Data Distribution Normal & Pre-Fire .....	85
Figure 62: Ionization Signal Algorithm Performance .....	86
Figure 63: Ionization Analog Signal Threshold Analysis.....	87
Figure 64: Experiment 11 Ionization Alarm Performance Comparison.....	88
Figure 65: Algorithm Logistical Flow Chart .....	89
Figure 66: Multi Sensor Algorithm Performance .....	91
Figure 67: Simplified Algorithm Logistical Flow Chart .....	92
Figure 68: Simplified Multi Sensor Algorithm Performance .....	92



## Chapter 1: Background

Cooking related equipment fires continue to be the leading cause of fires in homes in the U.S. The National Fire Protection Association (NFPA) tracks home fire data where the fire department was responded in the National Fire Incident Reporting System (NFIRS). The NFPA report on home structure fires between 2007 and 2011 suggests 43% of home fires originate in the kitchen due to cooking equipment, causing an average of 38% of the injuries (Figure 1). This equates to annual averages of approximately 176,000 fires and 5,000 injuries (Ahrens, 2013).



**Figure 1: Leading Causes of Home Structure Fires 2007-2011 (Ahrens, 2013)**

The Consumer Product Safety Commission (CPSC) conducted a phone survey between 2004 and 2005 in an effort to determine the number of unreported residential fire incidents. Data from this survey suggests that the actual number of cooking related fires is more than fifty times the number of reported fires (Greene, et al., 2009) many however go unreported.

To understand the cooking fire problem, a comparison of structure fire trends with cooking fire trends is provided. A review of the fire incidents in residential structures shows structure fires have been decreasing steadily since 1997, as seen in Figure 2 from the NFPA report on “Trends and Patterns in U.S. Fire Losses 2011” (Levesque, 2013). Data from 1977-2011 indicates fire incidents decreased by 51% in a steady downward trend. Likewise, the number of cooking related fires reported over a similar time period shown in Figure 3 indicate a downward trend from 1980-1998 (Ahrens, 2012). Incomplete data exists for the 1999-2001 time period. The new version of the NFIRS released in 2002 allowed for easier input of minor fires such as cooking fires. As a result the number of incidents returned to the level seen in 1980. Although the trend in the U.S. for the last several decades has been one of decreasing fire incidents, the number of cooking related fire incidents remains steady, if not increasing. A comparison of the two statistics illustrates that cooking fires represented 20% of all home structure fires in 1977, whereas in 2011 cooking related fires represented over 40% of the all home structures fires. This continued increase in the percentage of home structure fires related to cooking indicates the need for increased research in the prevention of cooking related fires.

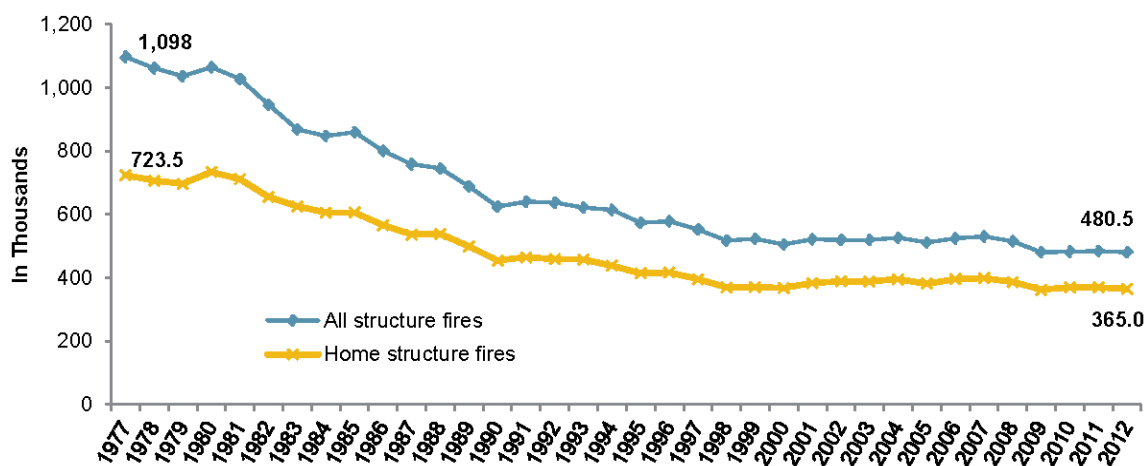


**Figure 2: U.S. Fire Incident Trends (in Thousands) 1997-2011 (Levesque, 2013)**

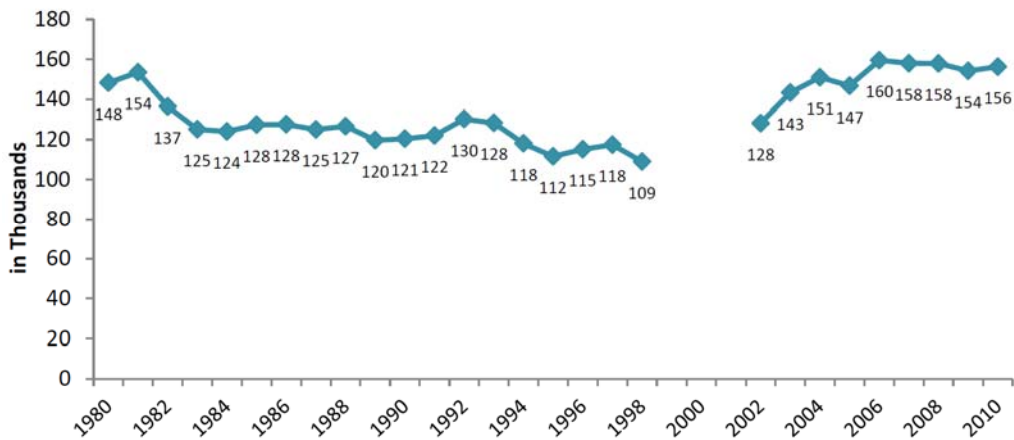


**Figure 3: Cooking Related Fires (in Thousands) 1980-2010 (Aherns, 2012)**

In 2013 the Federal Emergency Management Agency (FEMA) published the Topical Fire Report Series on Cooking Fires in Residential Buildings based on data obtained through the NFIRS to address specific U.S. fire problems. According to NFIRS data, an estimated 164,500 cooking related fires occurred annually between 2008 and 2010. Cooking related fires caused an average of 3,535 injuries and represented an average of \$307 million dollars in property loss. In addition to fire classification data, NFIRS also includes the leading cause of cooking related fires. For those incidents where a contributing factor was noted, “operational deficiency” was the leading factor in 60.3% of the fires, followed by “misuse of material or product” for 28.4% of the fires. Of all incidents where a contributing factor was noted, unattended equipment was noted in 43% of them (Federal Emergency Management Agency, 2013).

A phone survey sponsored by NFPA and conducted by Harris Inc. indicates smoke alarms, the current method of alerting occupants to a fire, are found in 96% of U.S. Homes (Aherns, 2011). This data does not match with the number of smoke alarms present in cooking related fires.

According to the FEMA study, 66.2% of the cooking fires had smoke alarms present when the fire was not confined to the room of origin. (Federal Emergency Management Agency, 2013), indicating that smoke alarms are located in areas of the home which are distant from the kitchen.

Work by the NFPA shows that missing or disconnected batteries account for three in five fires in which a smoke alarm was present but failed to sound (Aherns, 2011). In 1994 the CPSC did a phone survey of smoke alarm operability in residences. Respondents were asked about the presence of detectors, the location and to test them for functionality. The results indicated 11 % of homes had at least one inoperable smoke alarms with over 43% of them inoperable due to a removed or disconnected battery. The most common reason for removing the batteries was due to unwanted alarms or nuisance alarms which accounted for 32% of the alarms with missing or disconnected batteries (Smith, 1994).

With 43% of cooking related fires being unattended incidents, notifying occupants after the fire has occurred may be ineffective or too late for appropriate intervention. The need for an alarm specifically designed for residential cooking environments would permit the alarm to be located closer to the range providing additional notification to occupants. Work done by the National Institute of Standards and Technology (NIST) indicates frying bacon, broiling hamburgers and pizza and even boiling pasta can cause nuisance alarms during cooking (Bukowski, 2007).

Nuisance alarms occurring with current detection technology may lead to occupants removing smoke alarm batteries or even the smoke alarm themselves from the kitchen, increasing the time to alert occupants in the event of a cooking fire.

Cooking fires make up a significant proportion of fires within the home. In these fires unattended cooking is the leading factor contributing to the transition from cooking to fire. Current detection methodologies tend to result in nuisance alarms, which potentially result in their removal from the kitchen rendering them ineffective in cooking fire prevention. The need exists for a detection strategy with the capability of detecting an impending cooking related fire prior to it occurring while not resulting in a high number of false alarms. In theory this detection strategy would have the potential of intervening early enough to prevent the transition to fire without occupant interaction.



## Chapter 2: Previous Work

Cooktop fire detection has been researched over the past two decades starting with work done by the National Institute of Standards and Technology (NIST) in conjunction with the Consumer Product Safety Commission (CPSC). The goal of the three-phase project was to investigate pre-ignition conditions of cooking related fires. Phase I conducted at NIST evaluated the potential test scenarios by conducting testing on various food types, pan styles and range setups. A test enclosure equipped with range, cabinets and exhaust hood was constructed specifically for use in all three phases. The test procedure involved investigating unattended cooking by placing a sample pan/food combination on a burner in the “high” position and monitoring temperature, gas velocity, laser attenuation and FTIR gas analyzer for conditions approaching ignition of the food sample. This data was utilized to develop Phase II test samples and setups. Testing concluded that significant test variations in fire potential occur for different pan types, range types, and food types. (Johnsson, 1995)

Phase II of the NIST & CPSC study utilized the same enclosure to test food/pan configurations developed with the results of the phase I testing. Additional sensors including various types of smoke alarms were employed to determine the existence of pre-ignition signatures which could be utilized to detect a pre-ignition condition. The report suggested pan temperature and element temperature were the most effective indicators of a pre-ignition condition for food/samples with high oil/fat content. An evaluation of 26 tests concluded current smoke alarm technology was capable of identifying pre-ignition conditions for cooking fires, however, normal cooking also resulted in a significant number of nuisance alarms.

The work also addressed the potential thermal inertia of the electric heating elements. The removal of the power to the electric coil did not result in an immediate reduction in the food and pan temperature, conversely the temperature continued to increase for a period of time (Johnsson, 1998). The tests conducted included two with an empty pan, four with 100 ml (3.38 oz) of oil and four with 500ml (16.9 oz) of oil. The results of the tests are found in Table 1 including the maximum temperature that the pan contents reached prior to element shutoff and the time to reach the maximum temperature following shut off.

**Table 1: Pan Thermal Inertia Data (Consumer Product Safety Commission, 1998)**

Test Number	Amount of Oil (ml)	Pan Content Shut Off Temp (°C)	Time after shutoff to reach max oil temp (sec)
89	Empty	380	10
90	Empty	380	20
91	100	260	70
92	100	260	70
93	100	330	45
69	500	260	105
70	500	260	110
71	500	360	70
72	500	360	55

The results show that thermal inertia of the heating element caused the pan temperature to continue to increase for times ranging from 10 seconds to 110 seconds. The average time the pan temperature continued to increase was 59 seconds, with the time having a strong dependency on the amount of oil in the pan.

Phase III of the study occurred at the CPSC testing facility using the enclosure and cabinet setup from the NIST work with the addition of a low speed ceiling fan in the center of the room. Initial testing confirmed the reproducibility of cooktop fire testing between the earlier NIST work and

the CPSC work. Additional scenarios were tested based on input from manufacturers to evaluate cooking techniques not conducted in the Phase I and Phase II work which included caramelized sugars and flambé. Phase III of the study further reinforced the recommendations from Phase I and II for the use of a pan bottom temperature as a criterion for pre-fire conditions suggesting pan temperature be limited to approximately 340 °C (644 °F). The inclusion of an exhaust hood and ceiling fan were found to have an adverse effect on the gas concentrations with reductions exceeding 10%. Smoke alarm response was sporadic and did not provide a reasonable signal for pre-fire conditions. Recommendations were to include further work on adjustments in sensitivity for current smoke alarm technology to determine if pre-fire conditions could be detected with reasonable certainty and minimal false activations. (Consumer Product Safety Commission, 1998)

Additional work done at NIST evaluated “Smoke Alarm Performance in Kitchen Fires and Nuisance Alarm Scenarios.” The project focused on evaluating the response of smoke alarm performance during normal cooking scenarios along with the severity of various fire scenarios. Tests replicated toaster use, pan frying, broiling and oven use. Observations from the tests with commercially available ionization, photoelectric and multi-sensor alarms noted that ionization alarms had a higher probability of nuisance alarms for the cooking scenarios chosen. The probability of a nuisance alarm decreased as the distance from the cooking source increased. The level of alarm sensitivity was evaluated; however, no discussion was given to the potential of alarm threshold as it related to nuisance alarms. (Cleary, et al., 2013)

Published in 2007, NIST conducted research on smoke alarm nuisance alarms which included several cooking related operations. The work first evaluated the threshold level of smoke alarms through the use of NIST's fire-emulator/detector-emulator which was used to evaluate alarm response to smoke produced from various sources. After threshold levels were determined, nuisance alarm testing was performed for many of the common sources of nuisance alarms in the home, including those related to cooking. The test setup included a manufactured home and a two story home. Nuisance alarm testing involved both normal cooking and potential hazard scenarios for which alarm values were recorded. Data was available for alarm time; however, little data was recorded for the threshold values found in normal cooking. Photoelectric type smoke alarms showed less potential for nuisance alarms than the other alarm types. Both ionization and photoelectric type of smoke alarms produced nuisance alarms in most scenarios. (Bukowski, 2007)

In 2012 the University of Maryland conducted research on the "Response of Smoke Detectors to Smoldering Fires and Nuisance Sources." This work, sponsored by the Maryland Industrial Partnerships (MIPS) and USI Electric, considered four cooking scenarios in addition to two other household nuisance sources and compared the propensity of five different alarm technologies to alarm when exposed to a nuisance source. The four cooking sources included making toast, cooking onions, hamburgers and vegetable oil on a hot plate in the corner of a 5.49m (18ft) x 7.32m (24ft) room. Smoke alarms were arrayed on the ceiling in an arc 2.13m (7ft) from the cooking corner. The five alarm technologies included combination photoelectric/ionization sensors, carbon monoxide-ionization sensors, photoelectric sensors, ionization sensors and advanced algorithm ionization sensors. The results of the four cooking nuisance sources showed the advanced algorithm smoke alarms performed on par with photoelectric alarms for all four

cooking fire scenarios. Ionization type smoke alarms had the highest propensity for unwanted and nuisance alarms (Feng, et al., 2012).

The Fire Protection Research Foundation and NIST sponsored a 2011 study on “Home Cooking Fire Mitigation: Technology Assessment” conducted by Hughes Associates. The study evaluated the current technologies available both on the market and as research concepts which could be utilized to detect, prevent, or suppress home cooking appliance fires. Each technology was assigned a Fire Protection Effectiveness (FPE) number which represented a statistical analysis of the “potential percentage of fire losses that could be reduced through the application of a mitigation technology”. Scores ranged from zero to ten where a score of zero related to the technology having no impact and a score of ten related to the technology being capable of eliminating 100% of the losses. The FPE of sprinkler suppression showed the most promise based on the available data. With respect to detection technologies smoke detection stood above all other ignition prevention mechanisms with a user controlled burner temperature or utensil contact having the next best FPE. The study also identified gaps in the data used to develop the FPE, specifically the available data to identify the reliability of each specific technology and indicated further research was needed to determine the most effective technology (Dinaburg, et al., 2011).

In addition to the work on cooking fire detection previous work has been done on the use of gas sensors to identify fire signatures. A two phase project at the University of Maryland first by Denny in 1993 and again by Hagen in 1995 looked at the use of gas sensors for the detection of fires. Initial work by Denny looked at the feasibility of the sensors to detect a fire in small scale

bench experiments in the UL 217 Smoke Box. The second phase by Hagen looked at large scale experiments in a 3.65m (12 ft) by 3.65m (12 ft) by 2.44m (8 ft) high room. The gases evaluated were CO<sub>2</sub> and CO along with general values from Taguchi gas sensors. The work found the gas sensors are capable of distinguishing between flaming, smoldering fire conditions along with nuisance sources. The algorithm developed shows potential to reduce the time to activation of fire sensors while also reducing the number of nuisance alarms. (Hagen, 1994)

## Chapter 3: Experimental Setup

### 3.1 Kitchen Setup

An ongoing experiment in the Effectiveness of Fire Service Horizontal Ventilation and Suppression Tactics provided a two story modular home constructed in the large fire lab at the Northbrook, IL Underwriters Large Fire Laboratory. The home had a floor area of 297.3 m<sup>2</sup> (3,200 ft<sup>2</sup>) with 4 bedrooms, 2.5 bathrooms and a total of 12 rooms. The home incorporated a two story open family room to the second floor. The interior of the home was fully finished with drywall walls and cement board ceiling and carpet flooring. No mechanical systems existed within the home nor were they simulated during the testing.

The kitchen was 5.49 m (18 ft) long by 6.10 m (20 ft) wide with 2.74 m (9 ft) ceilings for a total floor area of 29.73 m<sup>2</sup> (320 ft<sup>2</sup>). The kitchen was open to the two story family room. An opening at the left back of the kitchen, accessed the laundry area measuring 1.17 m (3 ft 10 in) wide with An additional opening at the left front accessed the dining room measuring 1.09 m (3 ft 7 in) wide. An inset on the left side of the kitchen contained the space for a refrigerator measuring 0.72 m (28.5 in) deep and 2.62 m (103 in) long. The floor plan for the kitchen is presented in Figure 4.

The kitchen was fully furnished with a countertop, range, dishwasher dining room table, cabinets and 1.27 cm (0.5 in) cement board floor to simulate a tile floor. The countertop was 1.27 cm (0.5 in) cement board to simulate a stone countertop. The cabinets were unfinished oak purchased at the local hardware store and located along the right and front walls as shown in Figure 4. The upper cabinets were 0.31 m (1 ft) deep by 0.91 m (3 ft) tall and the base cabinets were 0.61 m (2

ft) deep by 0.87 m (2.88 ft) high. The walls were double layer gypsum board with a 1.59 mm (0.062 in) base and a 1.27 cm (0.5 in) top layer. The walls were spackled smooth and painted with a white primer coat of paint through the house.

Two window openings were located at the back right corner of the kitchen and a double door opening was located at the front right. The window openings were 0.91 m (3 ft) wide and 0.76 m (2.5 ft) tall. The door opening was 1.83 m (6 ft) wide and 1.78 m (5.83 ft) tall. The openings were filled with 5.1 cm (2 in) x 10.3 cm (4 in) stud framed partitions with a gypsum wall board interior face. Although the windows and door were removable, they remained in place during all tests.

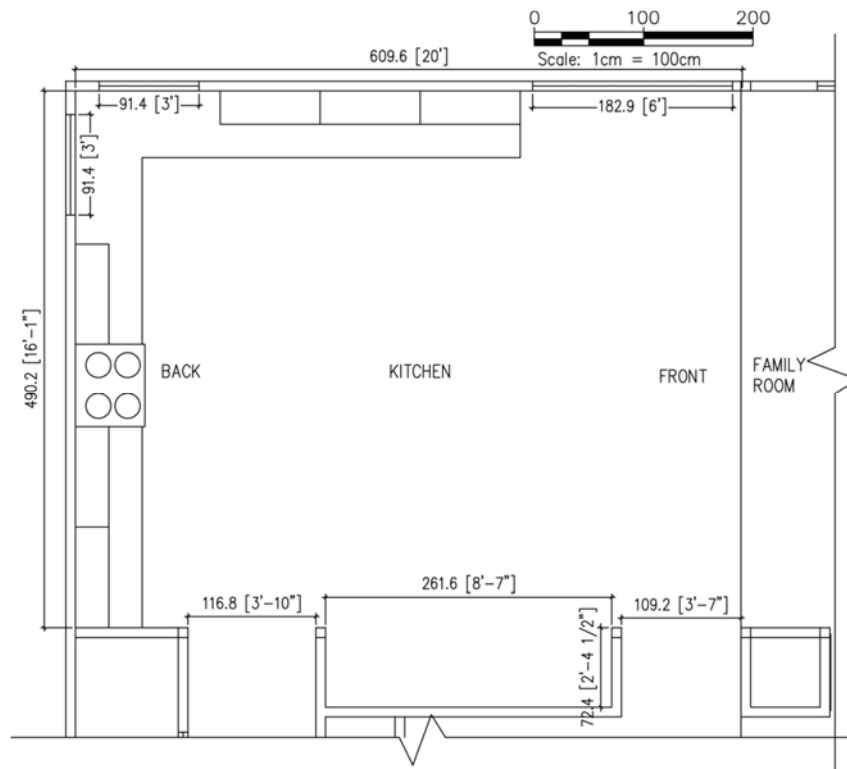


**Figure 4: Kitchen Layout**



### 3.2 Range Setup

A four burner electric range, purchased from a local home improvement store was used for the cooking experiments. The range measuring 0.76 m (2.5 ft) wide by 0.63 m (2.08 ft) deep and was centered on the back kitchen wall. All cooking was done on the front right 0.20 m (0.67 ft) electric coil burner rated at 2600 watts. A hood was located above the range however it was not operational during any of the tests. Power was provided to the range and the burner was controlled using the control knob located on the back of the range. See Figure 6 for the range set up.

### 3.3 Sensor Setup/Location

Several sensors were located on the range, above the range and in the kitchen. Sensors included thermocouple arrays, a Fourier transform infrared spectroscopy (FTIR) gas sampler, CO and CO<sub>2</sub> NDIR gas samplers, O<sub>2</sub> paramagnetic sampler, optical density sensors, heat flux gauges, CO detection, and several smoke detection technologies.

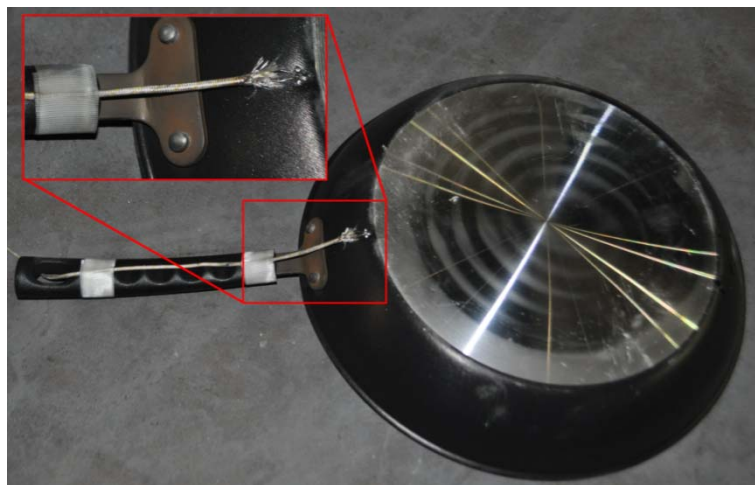


**Figure 5: Pan Thermocouple Position**

Thermocouples were located on the pan bottom via a welded bead type K thermocouple welded to the pan just below the handle (see Figure 5) intended to measure the pan temperature. In addition to pan temperature, a type K thermocouple probe was inserted at the center of the electric coil intended to contact the bottom of the pan (see Figure 7). This contact was not verified for each experiment so the sensor may have measured the air temperature near the center of the element. For those instances involving oil, a type K thermocouple probe was inserted in the oil to measure oil temperature. A thermocouple is comprised of a pair of wires of two alloys with a welded junction at the point of measurement. The voltage generated across the junction is proportional to the temperature along with the nature of the metals. This voltage can be measured to determine temperature in degrees.

A thermocouple array was centered above the pan at 30.5 cm (12 in), 66.0 cm (26 in) and 137.2 cm (54 in) above the range top using type K thermocouples. An additional type K thermocouple array was located 5.79 m (19 feet) away from the range measuring temperature at 30.49 cm (1 ft) increments between 30.5 cm (1 ft) and 243.8 cm (8 ft) above the finished kitchen floor.



**Figure 6: Range Sensor Setup**

The FTIR gas sampling point was located at 66.0 cm (26 in) above the range surface centered above the pan at the level of the exhaust hood. The sampling tube exited the kitchen through the front wall of the kitchen to FTIR equipment located on the exterior of the structure. A FTIR is uses infrared spectroscopy, the analysis of infrared absorption spectrum of a sample gas to identify the gas properties based on the wave numbers and peaks from the spectrum identified.



**Figure 7: Element Thermocouple**

CO, CO<sub>2</sub> and O<sub>2</sub> monitoring was accomplished through paramagnetic analyzers for oxygen and non-dispersive infrared (NDIR) analyzers for CO and CO<sub>2</sub>. The gas streams were run through ice water and dry ice to remove water from the samples prior to analysis. The copper sampling tube inlets were located 66.0 cm (26 in) above the range at the level of the exhaust hood. The sampling tubes exited the kitchen through the front wall to the exterior where the meters were located. Similar to the FTIR the NDIR also use infrared absorption to determine gas concentrations.

Optical density meters were utilized at 30.5 cm (12 in), 66.0 cm (26 in) and 137.2 cm (54 in) above the range surface. Three individual light sources were mounted at the corresponding sensor levels on a metal stand across from the sensors. Data was transmitted through the front wall to a data logger on the exterior of the structure. Optical density meters utilize a source light and a receiver to determine the amount of light obstructed over a give path length. This obstruction can be correlated to an optical density.

A single Gordon Gauge type water cooled heat flux gauge was located 66.0 cm (26 in) above the range at the hood level pointing down toward the centerline of the pan. The Gordon gauge, similar to the thermocouple uses the voltage created across two metal alloys in conjunction with a constant outer shell temperature to determine the amount of total energy absorbed.

Two analog CO detectors were utilized and the voltage signal from each monitored. One detector was located directly above the range surface on the ceiling and referred to as “Range Analog CO”. The other detector was located 5.79 m (19 ft) away from the range and referred to as

“Kitchen Analog CO”. Each detector was monitored for an alarm condition along with raw serial output data. The detectors on this work utilized electrochemical technology for detection CO. The sensing element incorporates an acid electrolyte solution and platinum electrodes. A current flow through the circuit is generated from a chemical reaction which occurs in the presence of CO.

Two analog ionization type smoke detectors were located alongside the CO detectors - one above the range and an additional unit 5.79 m (19 ft) away. The ionization smoke detector above the range was referred to as the “Range Analog Ion” detector and the detector located 5.79 m (19 ft) away was referred to as the “Kitchen Analog Ion” detector. These ionization sensors were monitored for an alarm condition along with raw serial output data. Ionization smoke detectors utilize a small amount of radioactive material which permits current flow through the chamber by ionizing the air within the chamber. Smoke particles entering the chamber decrease this current flow as they attach to the ions. Once the current flow has reached a pre-determined level the alarm activates.

Two commercially available combination smoke and CO detectors were also installed. These were located adjacent to the other detectors in the alarm array 5.79 m (19 ft) away from the range. The alarms, located opposite each other in the alarm array, were monitored for provided alarm and serial data (See Figure 8).



**Figure 8: Kitchen Smoke Alarm Array**

An additional five detectors were located in an array 5.79 m (19 ft) from the range; each alarm was monitored via the battery strength for activation. Serial analog data were not recorded for these alarms. This array included an ionization type, photoelectric type, combination photoelectric and ionization, combination photoelectric and CO and an advanced algorithm ion alarm. The advanced algorithm ion alarm combined an ionization sensor and microprocessor to eliminate nuisance alarms found in everyday cooking smoke and shower steam (Universal Security Instruments Inc., 2013). Photoelectric sensors contain a small light emitter and light sensitive device in their detection chamber. They can detect smoke through either light obscuration, whereas smoke enters the chamber it reduces the light seen by the receiver directly adjacent the source, or via light scattering whereas smoke enters the chambers it scatters the light pointed away from the light sensitive device towards it.

### 3.4 Video

Video was recorded from several vantage points in the kitchen. A camera was focused on the pan itself to capture the events taking place near the pan; a camera was focused on the range top to capture events taking place above the range and near the hood and a final camera was focused on

the front wall to capture the events taking place throughout the kitchen. In addition to video, thermal imaging was also utilized to visualize the temperatures surrounding the range. The thermal imaging camera was located adjacent the range top camera to capture events taking place above the range and near the hood.

### 3.5 Limitations

#### Pan Mass & Material

Materials used to make pots and pans vary greatly from metal to stone with various coatings to further heat transfer or provide anti stick qualities. These pan materials may have an impact on the precursor signal values produced and the action time required prevent transition to flaming fire. Tests of the various pan materials with a constant food source and cooking style would provide an indication how much of an effect pan materials have on the overall cooking fire transition process.

The size and mass of pans also varies greatly on today's market. Larger pans with more surface area have the potential to transfer more heat to the food while pans with a higher mass have more thermal inertia. The ability of the pan to transmit heat to the food will have direct implications on the transition to flaming fire and the time required to intervene before this transition occurs.

#### Kitchen Ventilation

None of the testing conducted evaluated the precursor signal values when the ventilation hood was active or additional ventilation was provided in the kitchen area by fans or mechanical heating/cooling equipment. Testing done by CPSC and NIST illustrated the impact ventilation of the cooking space has on alcohol sensors with variations of the values above 10% (Consumer

Product Safety Commission, 1998). An understanding of the effect of ventilation on the precursor signals identified is needed to validate the threshold values identified and limit nuisance activations. The ventilation style such as overhead hood and down draft designs may produce variations in the signal intensity and effect threshold values.

### Range Heat Source

The testing all utilized an electric range which is not the only commercially available cooking range. Gas cook tops, induction cook tops and glass cooktops are all additional heat sources which may have an effect on the thermal inertia of the pan. These variations in thermal inertia will impact the action time required to prevent the transition of flaming fire through either manual or automatic means.

### Sensor Location

The sensors in the test which show capabilities of detecting impending cooking fires were located various distances from the range top vertically as well as the pan centerline horizontally. The locations of these sensors have a direct impact on the values recorded as seen in the ionization signal strength above the range versus the ionization signal strength remote to the range. Further testing is needed to identify the optimum sensor placement to predict impending cooking fires while ignoring normal cooking practices.

### 3.7 Experiments

Eleven different cooktop fire scenarios were selected to evaluate a range of normal cooking and pre-fire conditions. The scenarios are listed in Table 2 along with the date of the test. Several experiments were conducted as both normal cooking followed by a simulated walk away incident resulting in a hazardous condition.



**Table 2: Cooking Fire Experiments**

Experiment Number	Test Date	Description
1	3/7/12	Lean ground beef – burn
2	3/7/12	Lean ground beef
3	3/7/12	Blackened fish (false positive check)
4	3/7/12	Vegetables – blackened and then burnt
5	3/7/12	Seared steak (False positive check)
6	3/8/12	Bacon
7	3/8/12	Bacon - Burn
8	3/8/12	Corn Oil
9	3/8/12	Corn Oil
10	3/8/12	Peanut Oil w/ French fries
11	3/8/12	Oven Mitt

Experiment 1

The lean ground beef, experiment 1, consisted of approximately 454 g (1 lb) of ground beef being placed in a pan. The heating element was set to high and a simulated unattended cooking event was conducted. The ground beef was left on high for 20 minutes and 20 seconds when the range was shut off and the data logging ceased without ignition. The experiment is illustrated in Figure 9(a) through Figure 9(e) at 5 minute increments. The ground beef was still raw (reddish pink color) on top however a layer of char had formed on the bottom (Figure 10).

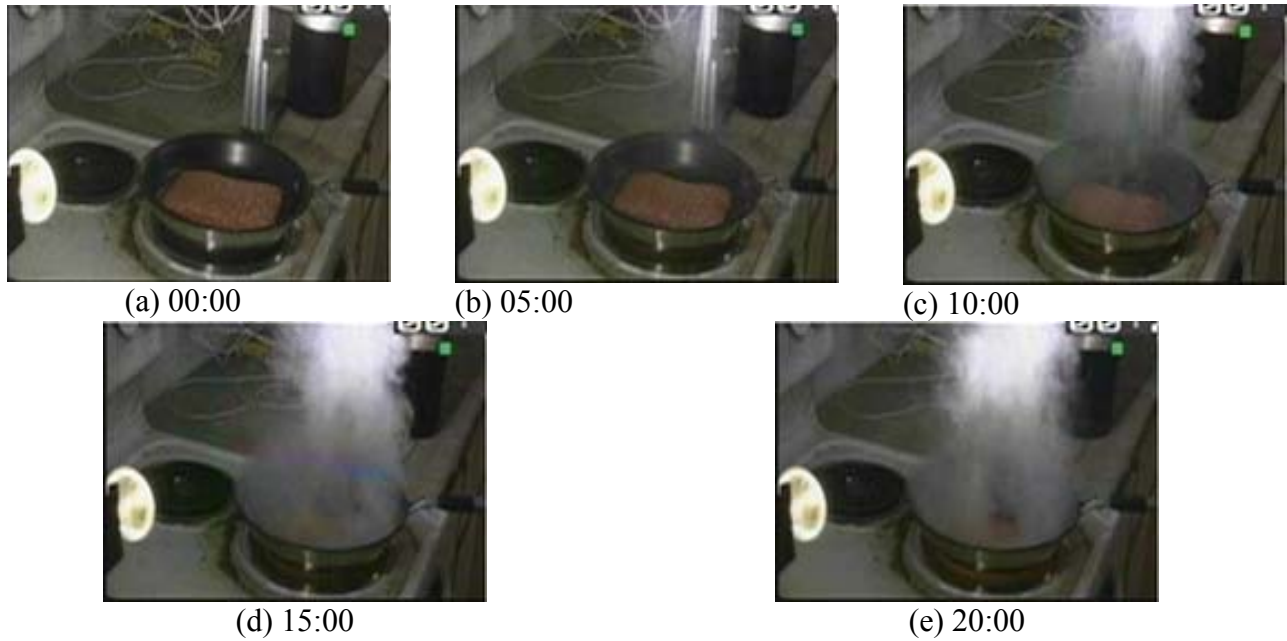


**Figure 9: Experiment 1 – Chronological Images**



**Figure 10: Experiment 1 – Ground Beef Result**

### Experiment 2

Lean ground beef was also browned using normal cooking practices for experiment 2. The approximately 0.45 kg (1 lb.) of ground beef was spread evenly in the bottom of the pan and the element was turned to high. At 117 seconds the beef was flipped and stirred until 395 seconds, when the heat was turned off. The beef was stirred additionally to avoid burning as the element cooled and was removed from the heat at 480 seconds. The experiment is illustrated in Figure 11(a) through Figure 11(e) at the relevant time steps. At the conclusion of the experiment the

beef was scooped out of the pan and placed on a paper plate. The beef was brown in color and dry (see Figure 12).



**Figure 11: Experiment 2 – Chronological Images**



**Figure 12: Experiment 2 – Ground Beef Result**

### Experiment 3

The blackening of fish is one of the many cooking practices which may result in smoke production during normal cooking thus it was selected for experiment 3. The range element was set to the high position and the pan permitted to heat up. Two strips of white fish were placed in the pan one at a time to start the experiment. After 82 seconds and 84 seconds each of the fish were flipped. At 136 seconds the strips of fish were pressed into the pan using the spatula for approximately 1 second each and after a total of 154 seconds the strips were each removed from the pan one at a time. The pan was scrapped with the spatula to dislodge anything stuck to the pan from the first two strips and at 174 seconds and 176 seconds two additional strips were added to the pan. The second set of strips was flipped after 96 seconds of blackening at 272 seconds into the test. After an additional minute and 14 seconds the heat was switched off and the second set of strips was removed from the pan and placed on a paper plate. Experiment 3 is illustrated in Figure 13(a) through Figure 13(i) around the experiment times discussed above. The resultant fish had an opaque white color with blackened char as illustrated in Figure 14.

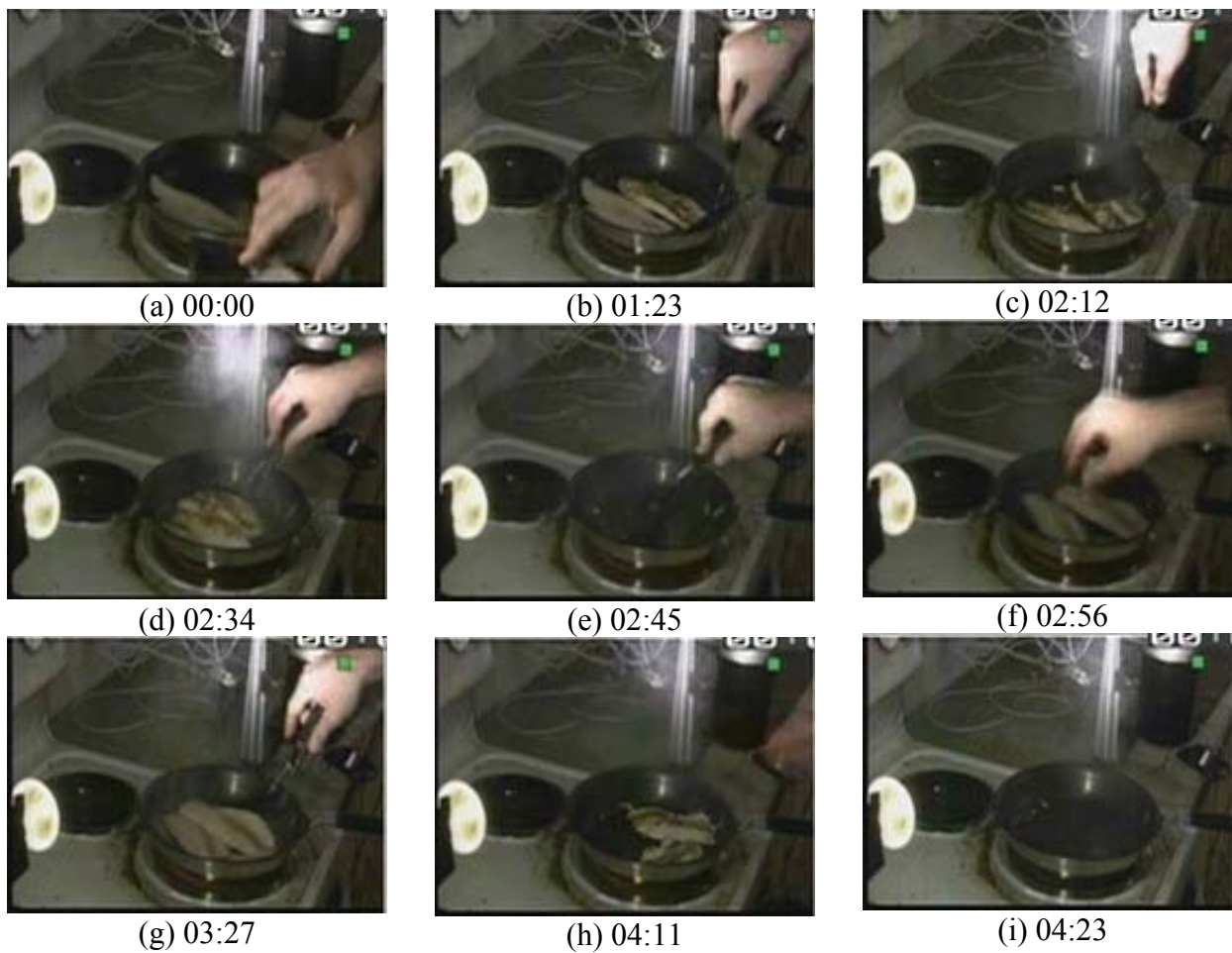


**Figure 13: Experiment 3 – Chronological Images**



**Figure 14: Experiment 3 – Blackened Fish Result**

#### Experiment 4

The blackening of vegetables followed by a simulated unattended cooking incident was conducted in experiment 4. A small amount of oil was placed in the bottom of the pan and the range element was set to high. After allowing the pan to heat up for 2 minutes and 36 seconds the 908 g (2 lb) bag of mixed vegetables was added to the pan. The vegetables were stirred to prevent them from burning to the bottom of the pan until 7 minutes and 32 seconds into the experiment when unattended cooking was simulated. The vegetables were left on the element set to high for 9 minutes and 15 seconds (16 minutes and 48 seconds experiment time) before enough of the water had evaporated from the pan for it to slightly elevate of the burner. The experiment continued until 22 minutes and 3 seconds when the vegetables were removed from the range element. Experiment 4 is illustrated in Figure 15(a) through Figure 15(k) through normal cooking and at the various intervals discussed above. The result of the first 7 minutes and 32 seconds of the experiment was a colorful pan of vegetables and after 22 minutes and 3 seconds the vegetables were charred black in color, Figure 16.



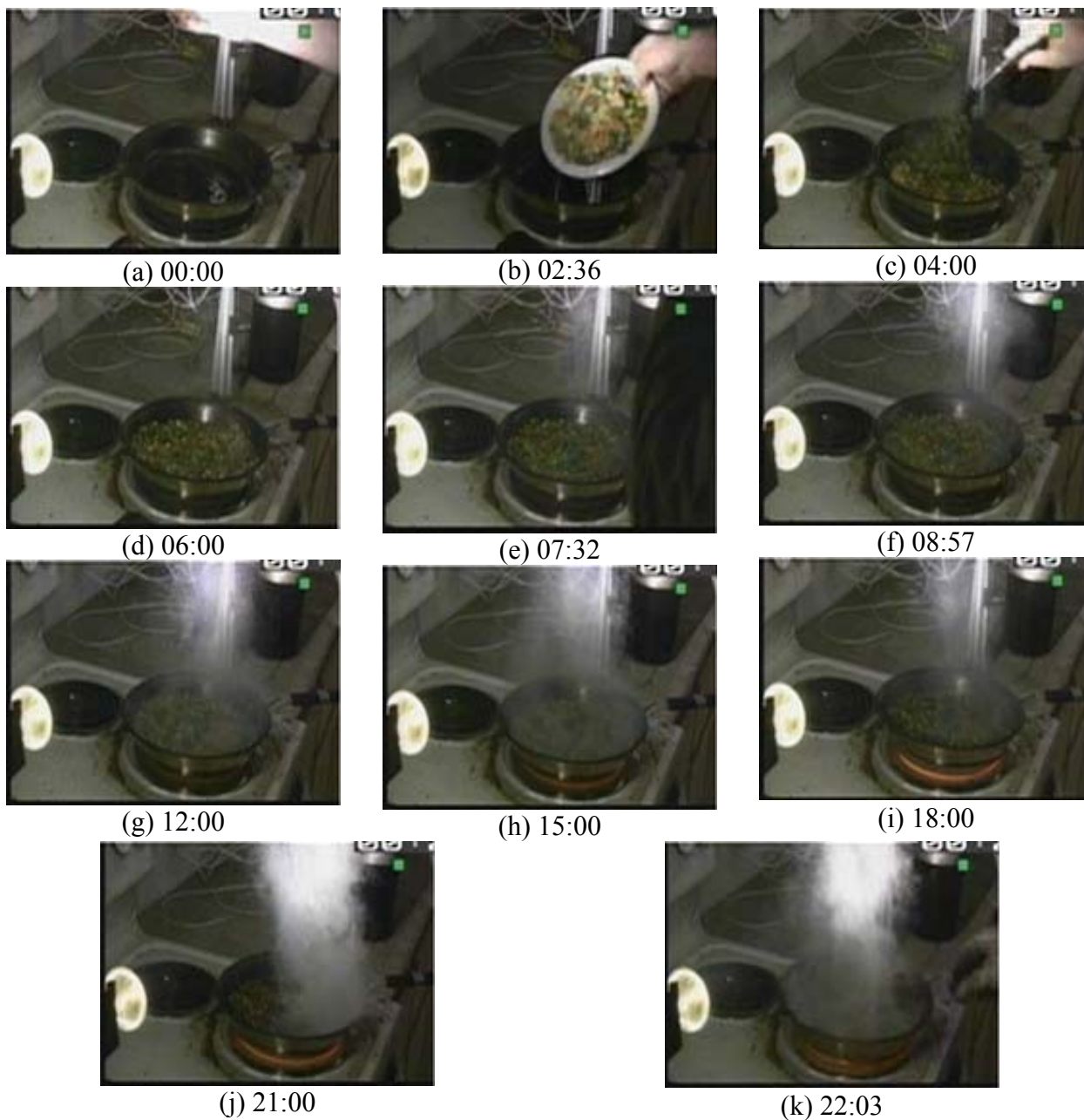


**Figure 15: Experiment 4 – Chronological Images**



**Figure 16: Experiment 4 – Vegetables Result**

## Experiment 5

The searing of steak was conducted for experiment 5 with two petite sirloin steaks measuring approximately 3 cm (1.25 in) thick and weighing approximately 340 grams (0.75 lb). The pan was placed on the range element and the setting adjusted to high, allowing the pan to heat up for 3 minutes and 35 seconds. The steaks were added to the pan one at a time and allowed to sear on one side for 4 minutes and 27 seconds (8 minutes and 5 seconds from the start of the experiment) when they were then turned one at a time. The opposite side was allowed to sear for 2 minutes and 58 seconds when the first steak was removed from the pan (11 minutes 3 seconds experiment time). The second steak seared and additional 53 seconds and was removed at 11 minutes and 56 seconds experiment time. Experiment 5 is illustrated in Figure 17(a) through Figure 17(f) at the times intervals discussed. The resulting steak was blackened on the top and bottom but red in the middle (“black and blue”) as seen in Figure 18.

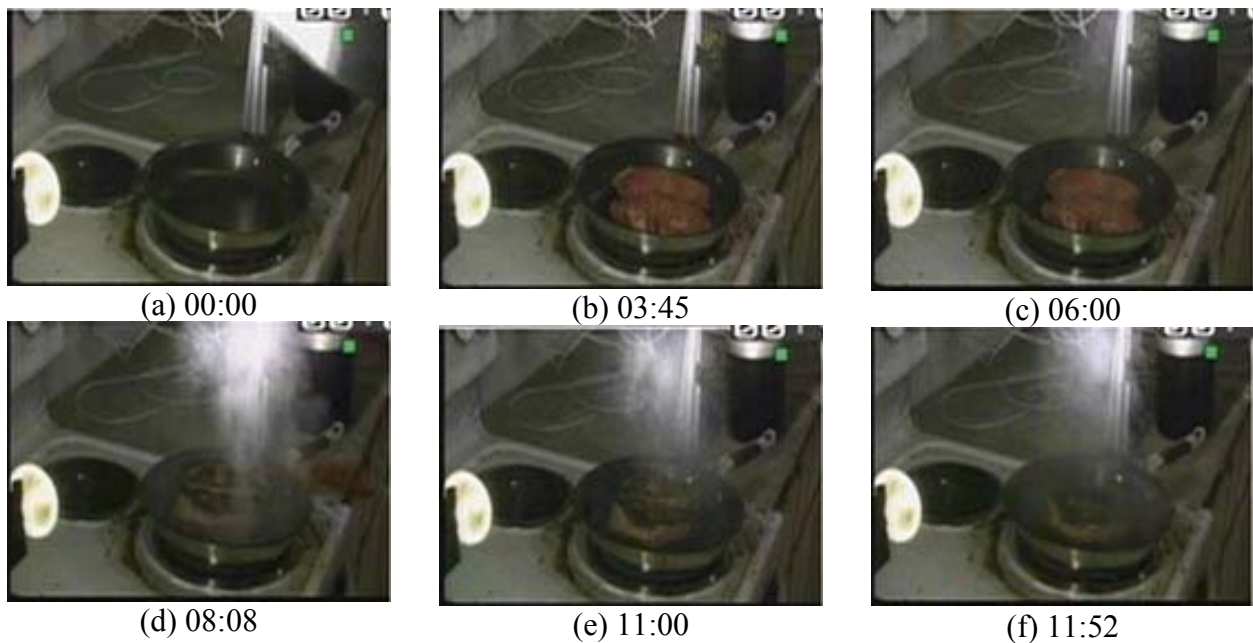


**Figure 17: Experiment 5 – Chronological Images**





**Figure 18: Experiment 5 – Seared Steak Result**

### Experiment 6

Experiment 6 tested the response to normal bacon cooking of the experiment sensors. Bacon strips were laid evenly in the frying pan so as to avoid overlapping strips. The pan was placed on the range element and the element heat set to the high setting. The bacon was heated without interaction for 2 minutes and 10 seconds then it was flipped and moved in the pan to prevent burning until it was removed from the pan at 6 minutes and 40 seconds. The pan remained empty for 10 seconds and at which time additional strips of raw bacon were added to the pan one at a time until the pan bottom was covered in bacon with no concern for overlap or keeping the bacon flat. After the second batch of bacon was cooked by stirring and flipping for 2 minutes and 39 seconds the bacon was removed from the pan and only the grease remained. A simulated unattended cooking incident was initiated as if the occupant neglected to shut off the element and walked away from the range. Approximately 5 minutes after the simulated unattended cooking incident was initiated, i.e. at 15 minutes and 2 seconds into the test, the grease in the pan autoignited. Experiment 6 is illustrated in Figure 19(a) through Figure 19(m).



(a) 00:00



(b) 02:10



(c) 04:00



(d) 06:37



(e) 06:50



(f) 07:35



(g) 09:00



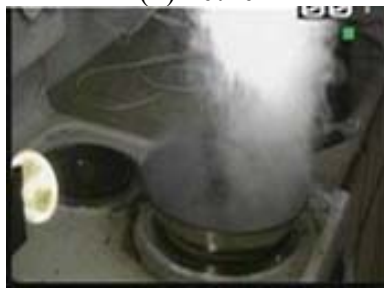
(h) 10:10



(i) 12:00



(j) 14:00



(k) 14:50



(l) 15:03



(m) 15:25

**Figure 19: Experiment 6 – Chronological Images**

## Experiment 7

Bacon was again used in experiment 7 to simulate an unattended cooking event where bacon was placed in a pan on the range with the burner element set to high and left unattended. A 454 g (1.0 lb) package of bacon was placed in the pan and the pan was placed on the range element as depicted in Figure 21. The element was set to the high setting with no other intervention. At 23 minutes and 4 seconds into the test the bacon in the pan autoignited. The progression of the experiment is illustrated in Figure 20(a) through Figure 20(h) showing the progression to flaming fire.

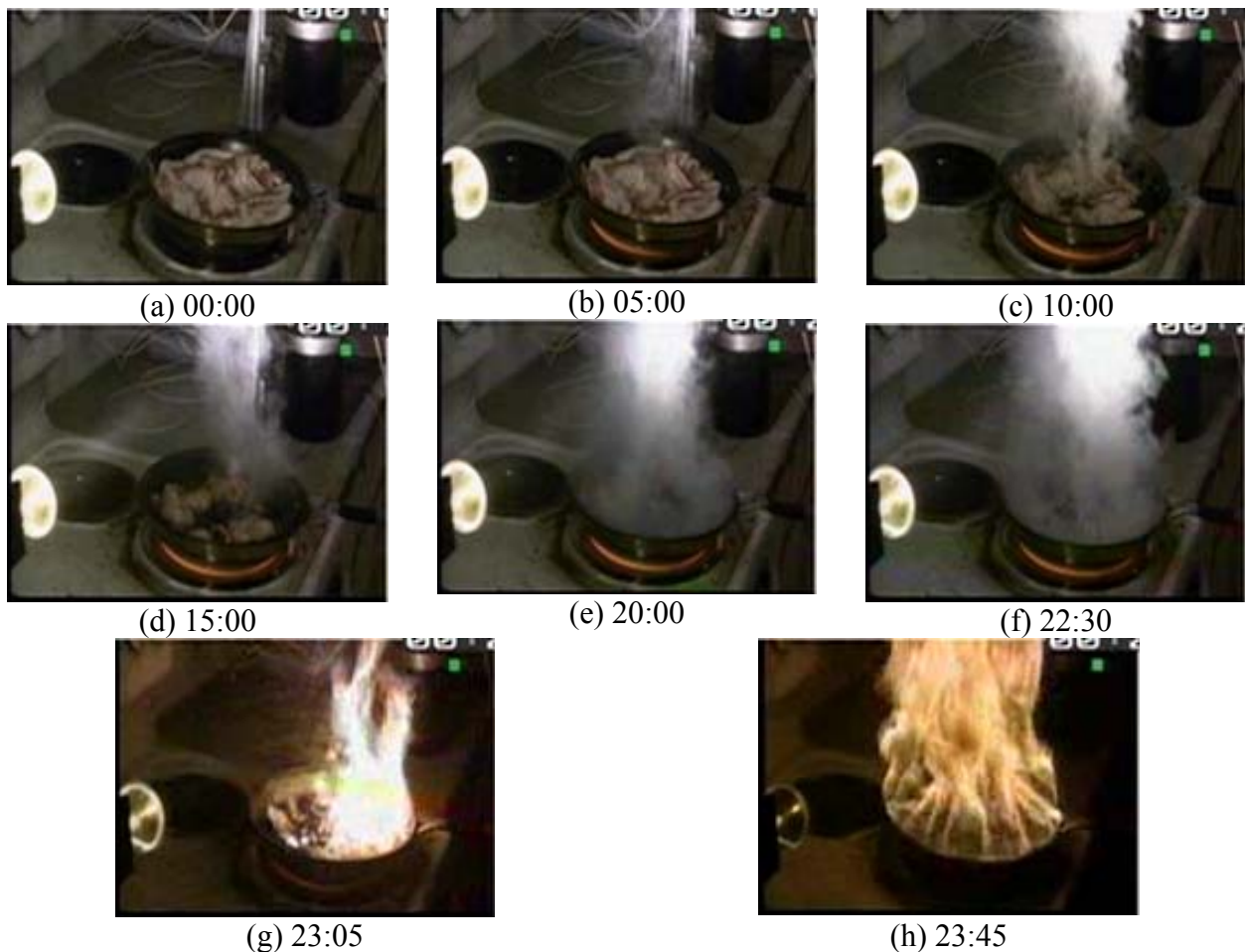


**Figure 20: Experiment 7 – Chronological Images**



**Figure 21: Experiment 7 – Bacon Start**

#### Experiment 8 and Experiment 9

Corn oil was utilized in experiment 8 and experiment 9 as simulated, unattended cooking incidents. Approximately 1.9 cm (0.75 in) of oil was poured into the pan and the pan placed on the range element. The element was placed on the high setting and simulated, unattended cooking was conducted. The oil was heated by the element till it reached its autoignition temperature at 13 minutes and 23 seconds for experiment 8 and 10 minutes and 2 seconds for experiment 9. Experiment 8 is illustrated in Figure 22(a) through Figure 22(g) and experiment 9 is illustrated in Figure 23(a) through Figure 23(g).



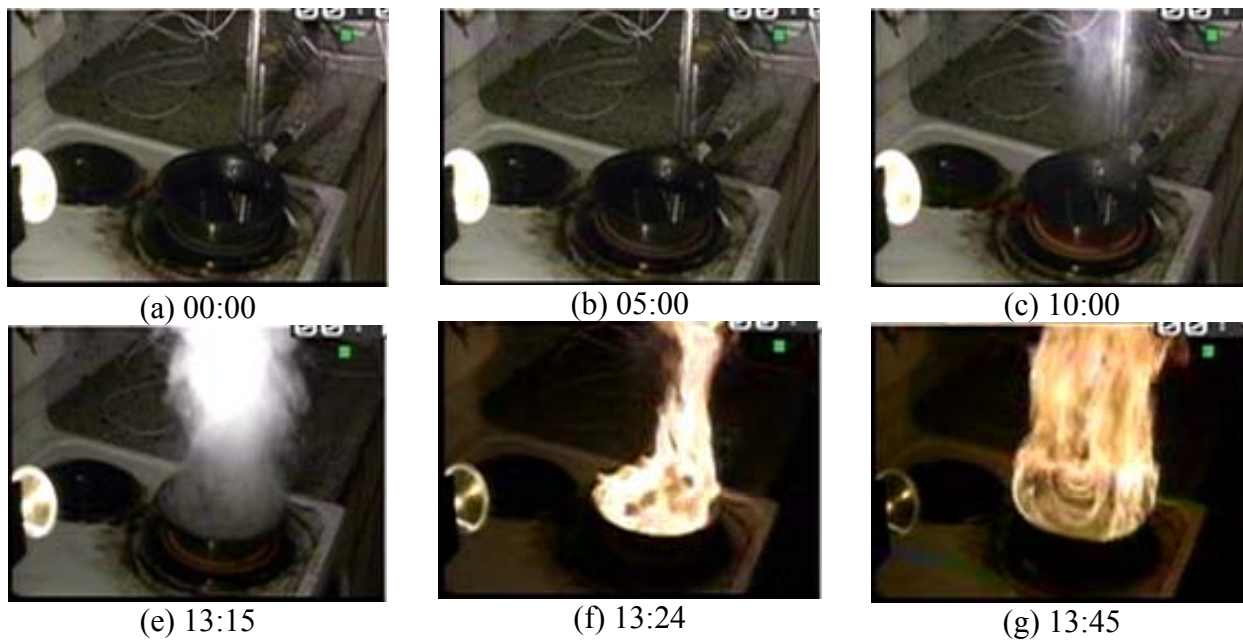


**Figure 22: Experiment 8 – Chronological Images**

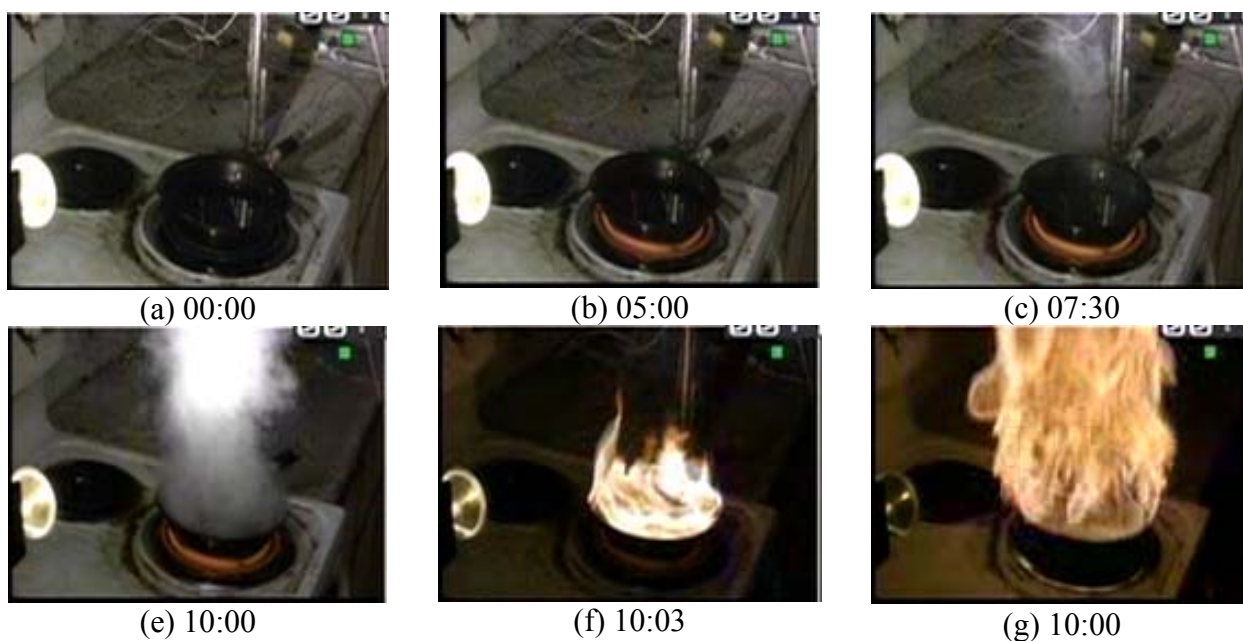


**Figure 23: Experiment 9 – Chronological Images**

## Experiment 10

Peanut oil was used to cook French fries in experiment 10 for both normal cooking and a simulated unattended cooking incident. A pot was filled 3/4 of the way with peanut oil and placed on the range element. The element was set to the high setting and the oil was permitted to heat for 15 minutes and 24 seconds while being stirred at various intervals to ensure uniform heating. At 15 minutes and 24 seconds a handful of French fries (i.e. approximately 35 French fries), was dumped from a plate into the oil and no other interaction occurred until the French fries and oil autoignited at 37 minutes and 12 seconds into the test. The flaming fire continued until 37 minutes and 51 seconds when the lid was placed on the pot to extinguish the fire. The Pot was removed from the burner and permitted to cool. Figure 24 depicts the pan and oil set-up and amount of French fries prior to the start of the experiment. The experiment is illustrated in Figure 25(a) through Figure 25(i) at the various time intervals discussed above.



**Figure 24: Experiment 10 – Pan & French Fries Setup**

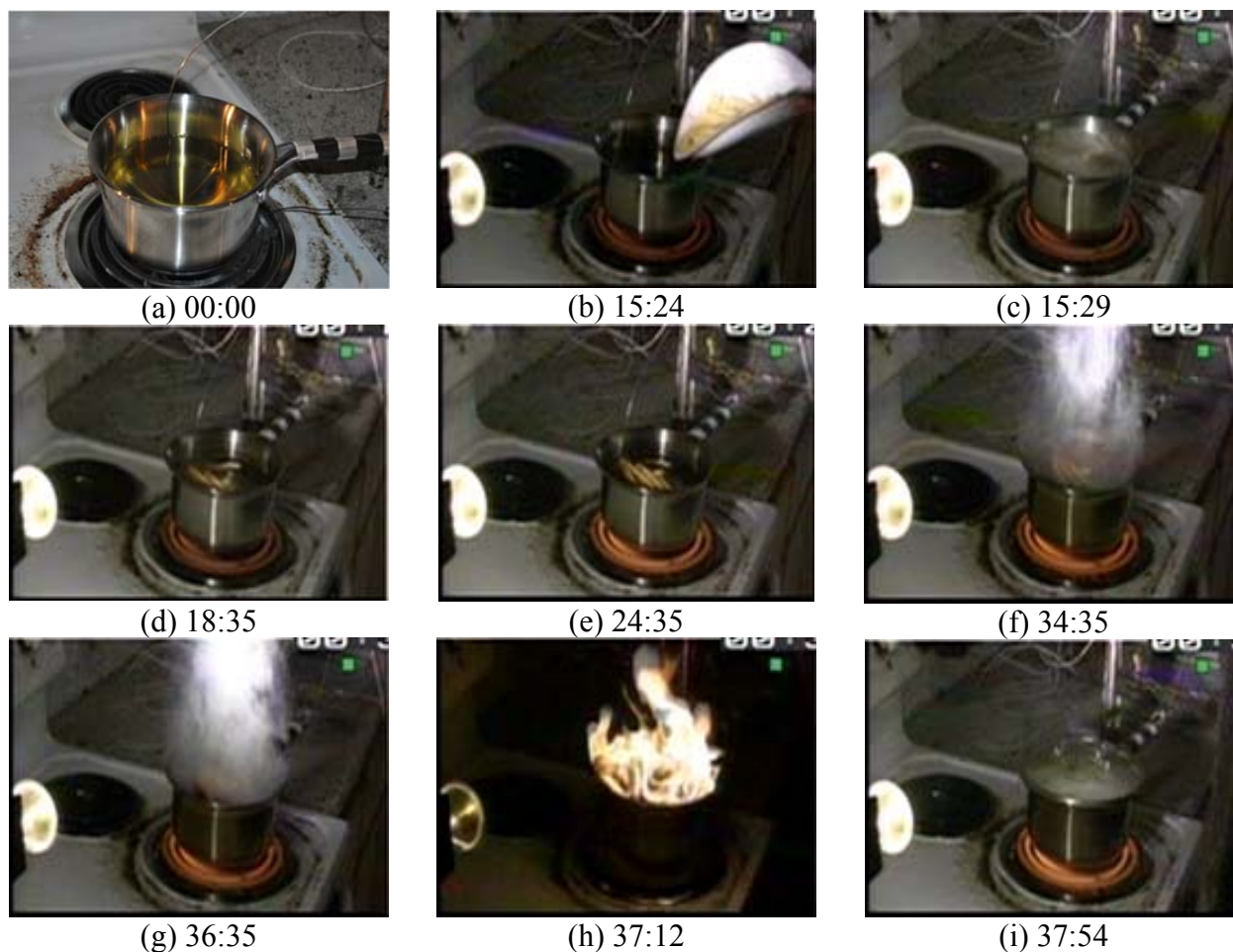


**Figure 25: Experiment 10 – Chronological Images**

### Experiment 11

Finally, for experiment 11 a pot holder was used to simulate a foreign object situated on the range element as the element was set to high. The cotton pot holder was placed on the range element and the element set on the high setting. The pot holder ignited at 1 minute and 2 seconds. Experiment 11 is illustrated in Figure 26(a) through Figure 26(f) below at 15 second increments.



(a) 00:00



(b) 00:15



(c) 00:30



(d) 00:45



(e) 01:02



(f) 01:15

**Figure 26: Experiment 11 - Chronological Images**



## Chapter 4: Data: Initial Analysis

### 4.1 Identification of Stages (Normal, Pre-Fire/Action, Fire)

Given that the intent of the research is to identify pre-cursors to cooking fires while limiting nuisance alarms. Thus, the data analysis in this chapter focuses on three stages of a cooking related fire. The normal cooking stage involves the various cooking styles, including activities which produce smoke and particulate potentially causing nuisance alarms when standard smoke alarm technology is installed near the cooking appliance. As ‘normal cooking’ is a subjective term, the indicators used to determine the bounds of normal cooking involved evaluation of the videos of the experiment. The limit of normal cooking was established subjectively based on personal experience. The time at which the experiment transitioned from normal cooking to a pre-fire stage is noted in

**Table 3** along with the justification for the point at which the transition was identified.

**Table 3: Normal Cooking Data Criteria**

Exp. #	Description	End “Normal” Cooking	Justification	Transition to Fire*
1	Ground Beef – Burn	0 s	Experiment intended to represent unattended cooking	N/A
2	Ground Beef – Brown	480 s	N/A	N/A
3	Blackened Fish	246 s	N/A	N/A
4	Vegetables – Black & Burn	456 s	Experiment started unattended cooking at 456 s.	N/A
5	Seared Steak	720 s	N/A	N/A
6	Bacon – Normal & Burn	605 s	All Bacon removed from pan, oil grease remained with element set to high.	902 s
7	Bacon - Burn	0 s	Experiment intended to represent unattended cooking.	350 s
8	Corn Oil	0 s	Experiment intended to represent unattended cooking.	803 s
9	Corn Oil	0 s	Experiment intended to represent unattended cooking.	602 s

10	Peanut Oil & French Fries	1104 s	French Fries cooked in oil for 3 minutes, maximum recommend time from package.	
11	Pot Holder	0 s	Entire experiment.	62 s

\* Transition to fire characterized by visually observing flame.

The action or pre-fire stage involves the specific area of interest for this research project intending to detect the precursors to a cooking fire early enough to provide sufficient time for a homeowner to take action to prevent a flaming fire from occurring. Actions by homeowners could include shutting off the range, or future developments may yield range/cooktops which do so automatically. The time needed for shutoff should consider the thermal inertia of the heating element for electric ranges where the temperature of the pan and its contents would continue to increase even though the element is turned off.

This was done through an evaluation of the CPSC study from 1998 which evaluated pan/element thermal inertia. The data was tested for normalcy with an Anderson-Darling test as shown in Figure 27, with a P-Value  $> 0.05$  indicating a normal distribution. A histogram of the CPSC data with a normal distribution curve fit to the data is presented in Figure 28 (Consumer Product Safety Commission, 1998).

Using one standard deviation, a range of 26.5 seconds to 91.5 seconds well encompasses 68.2% of the potential increases due to thermal inertia. The outlying values represent the empty pan on the lower end of the time of increase and a shut off temperature found in normal cooking styles at the upper end. For the results of this analysis detecting a fire prior to this time will theoretically permit intervention by activities such as removing the heat source to prevent

transition to fire. The range of 26.5 seconds to 91.5 seconds was utilized to classify the detection or pre-fire range in this study.

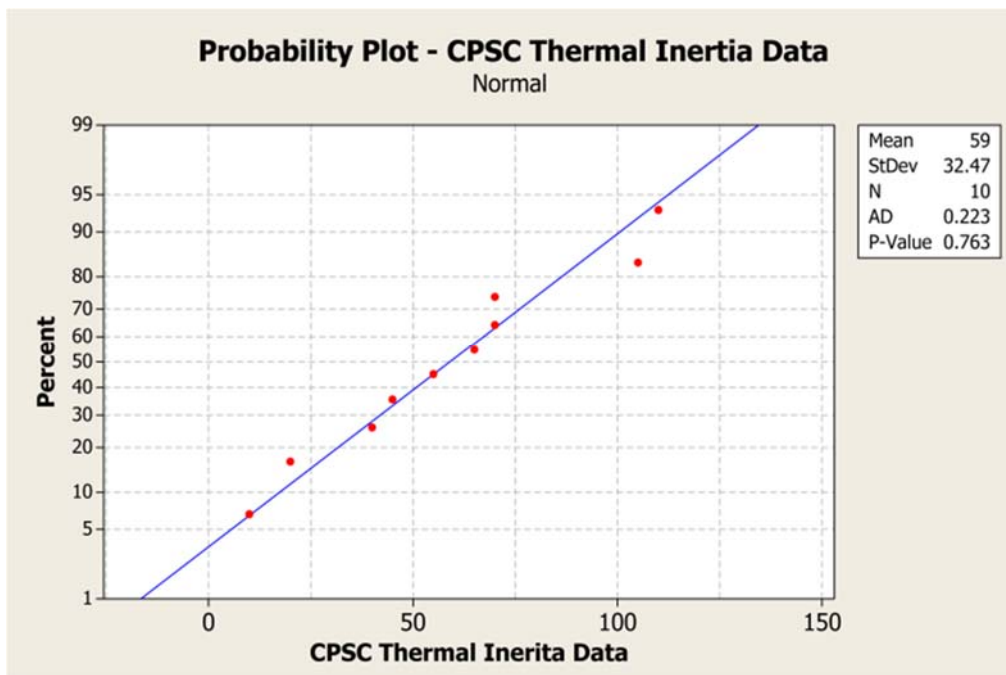


Figure 27: Anderson-Darling Probability Plot – CPSC Thermal Inertia Data

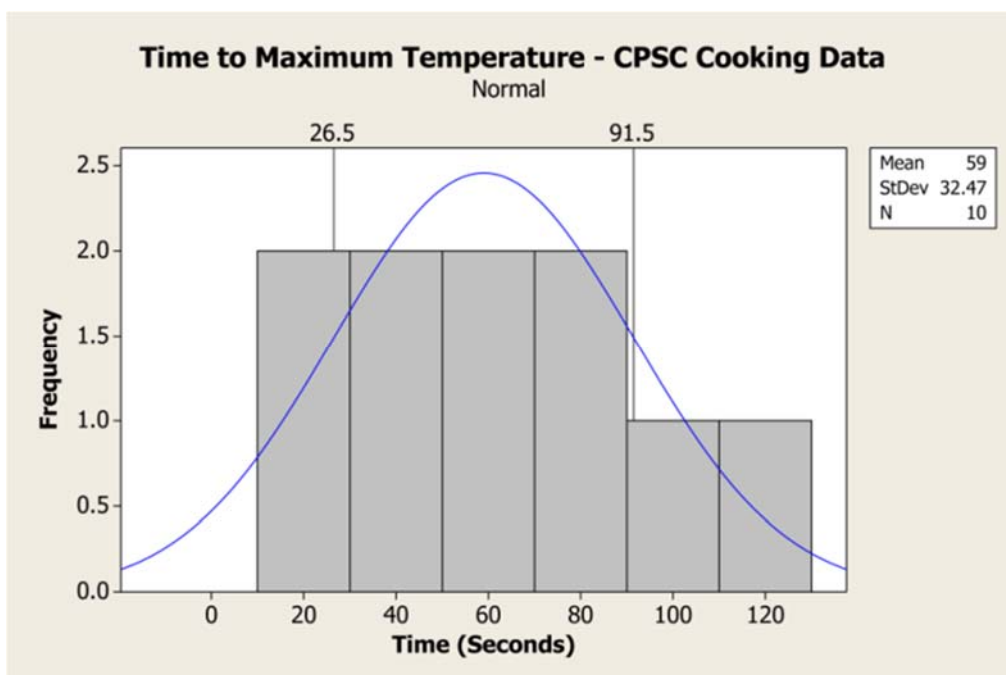


Figure 28: Time to Maximum Temperature Histogram & Normal Fit for CPSC Thermal Inertia Data

To classify the fire stage of the experiments in this study, video was evaluated to identify the time at which the first visible flame occurred within the pan. In all instances where transition occurred, the flame region encompassed the entire pan almost immediately following autoignition.

#### 4.2 Sensor Results

##### Pan Centerline Gas Temperature

Centerline gas temperature values above the range recorded for all of the experiments where normal cooking occurred were between 19.26 °C (66.57 °F) and 72.41 °C (161.3 °F). This range is comparable to that recorded during the pre-fire period of between 18.27 °C (64.89 °F) to 90.92°C (195.7 °F) and represents no noticeable difference between the centerline gas temperatures above the pan for normal cooking vs. the pre-fire stage. Many of the maximum temperatures reached in pre-fire conditions are also present in normal cooking experiments. The maximum temperature was highly dependent on the duration of heating, as seen in experiment 10, the experiment with the longest duration, where the maximum exceeded 90 °C (194 °F). The centerline temperature above the pan did not appear to provide any indication that an impending fire was approaching.

**Table 4: Centerline Pan Temperatures Minimum and Maximum for Normal and Pre-Fire – All Experiments**

Centerline Pan Temperature				
	Normal cooking		Pre-Fire	
Experiment Number	Minimum Temperature °C (°F)	Maximum Temperature °C (°F)	Minimum Temperature °C (°F)	Maximum Temperature °C (°F)
1	N/A	N/A	33.85 (92.93)	65.61 (150.1)
2	27.02 (80.64)	43.29 (109.9)	N/A	N/A
3	28.88 (83.98)	63.88 (147.0)	N/A	N/A
4	23.93 (75.07)	45.93 (114.7)	28.77 (83.79)	64.41 (147.9)
5	29.05 (84.29)	56.83 (134.3)	N/A	N/A

6	24.03 (75.25)	59.08 (138.3)	31.73 (89.11)	68.24 (154.8)
7	N/A	N/A	31.41 (88.54)	69.87 (157.8)
8	N/A	N/A	29.18 (84.52)	61.18 (142.1)
9	N/A	N/A	29.96 (85.93)	64.96 (148.9)
10	19.26 (66.67)	72.41 (162.3)	31.91 (89.44)	90.92 (195.7)
11	N/A	N/A	18.27 (64.89)	23.98 (75.16)

### Kitchen Gas Temperatures

Similar to the centerline pan temperature the temperatures recorded in the center of the kitchen were dependent on heating duration. Temperatures recorded during the normal cooking were also seen during the pre-fire stage. The minimum and maximum temperatures recorded along any point of the array during the normal cooking and pre-fire stages for the kitchen thermocouple array are provided in Table 5. The pre-fire values do not increase appreciably above the normal values and many of the pre-fire values include normal room temperatures. Kitchen temperature or ceiling mounted heat alarms do not appear to distinguish between normal cooking and pre-fire conditions and would result in nuisance alarms thus cannot be used as a reasonable precursor signal to an impending cooking fire.

**Table 5: Kitchen Thermocouple Array values Normal and Pre-Fire – All Experiments**

Kitchen Temperature				
Experiment Number	Normal cooking		Pre-Fire	
	Minimum Temperature °C (°F)	Maximum Temperature °C (°F)	Minimum Temperature °C (°F)	Maximum Temperature °C (°F)
1	N/A	N/A	22.15 (71.87)	29.19 (84.54)
2	21.53 (70.75)	25.56 (78.01)	N/A	N/A
3	21.67 (71.01)	26.76 (80.17)	N/A	N/A
4	21.86 (71.35)	26.50 (79.70)	22.05 (71.69)	28.61 (83.50)
5	21.82 (71.28)	27.50 (81.50)	N/A	N/A
6	22.14 (71.85)	27.86(12.15)	22.39 (72.30)	28.28 (82.90)
7	N/A	N/A	20.88 (69.58)	29.03 (84.25)
8	N/A	N/A	17.99 (64.38)	24.43 (79.97)
9	N/A	N/A	19.20 (66.56)	25.80 (78.44)

10	17.35 (63.23)	24.52 (76.14)	18.01 (64.42)	25.66 (78.19)
11	N/A	N/A	16.45 (61.61)	19.65 (65.37)

N/A – Not applicable

### Pan Temperature

As suggested by the NIST and CPSC research, pan temperature does have some ability to determine if a cooking scenario will transition to fire. If the temperature can be kept below the autoignition of the food being prepared, the ignition of the food will be prevented. As shown in Table 6, the pan temperature during the searing steak experiment (experiment 5) and blackening fish (experiment 3) never exceeded 330 °C (626 °F) for the normal cooking styles tested. This correlates to the theoretical maximum permitted pan temperature identified by CPSC of 340 °C (664 °F) (Consumer Product Safety Commission, 1998). Temperature increases of 60 °C (140 °F) or more over the normal cooking values are seen in the pre-fire conditions and action period.

**Table 6: Pan Temperature Normal and Pre-Fire – All Experiments**

	Normal Cooking	Pre-Fire
Experiment Number	Maximum Temperature °C (°F)	Maximum Temperature °C (°F)
1	N/A	519.18 (966.52)
2	154.31 (309.76)	N/A
3	329.00 (624.20)	N/A
4	Sensor Error	Sensor Error
5	316.48 (601.66)	N/A
6	326.17 (619.11)	384.10 (723.38)
7	N/A	582.83 (1081.1)
8	N/A	470.34 (878.61)
9	N/A	575.30 (1067.5)
10	206.17 (403.11)	373.71 (704.68)
11	N/A	N/A
Range	154.31 – 329.00 (309.76 – 624.20)	373.71 – 582.83 (704.68 – 1081.1)
Average	266.6 (511.9)	484.2 (903.6)

N/A – Not applicable

Figure 29 indicates the range of normal and pre-fire values for pan temperature for those experiments where a pan was utilized. There is a marked difference between normal cooking and pre-fire stages with no overlap indicating the pan temperature has the potential to serve as a precursor signal to cooking fires.

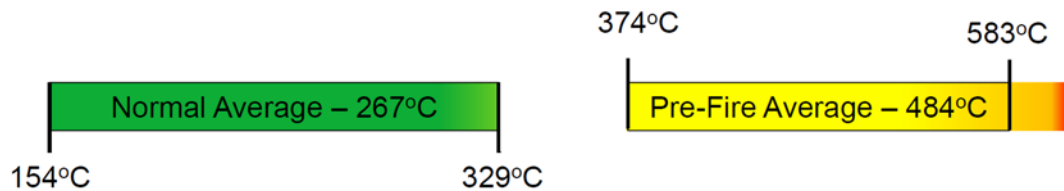


**Figure 29: Pan Temperature Range – Normal Cooking and Pre-Fire**

In addition to differentiating pre-fire conditions, the pan temperature did not illustrate nuisance alarm tendencies as the maximum temperature recorded during normal cooking was lower than any of temperatures recorded during the pre-fire detection periods. Pan temperature has the potential to serve as a precursor signal to an impending cooking related fire; however its potential impact on cooking styles and scenarios such as boiling water and cooking pasta was not tested during this work.

Monitoring pan temperature would involve a properly placed thermocouple in contact with the pan bottom surface as suggested in the work performed by CPSC (Consumer Product Safety Commission, 1998). In addition, the location of the thermocouple and lack of contact with the pan such as with a warped pan, may make the sensor record higher temperatures due to radiation from the heating element. This may eliminate some cooking styles difficult if the temperature was limited below ignition of many oils. Thus pan temperature as a precursor signal to an impending cooking fire may not meet the reliability desired in a cooking fire precursor signal.



## Element Temperature

Temperatures measured by the thermocouple probe placed at the center of the range element (see Figure 7 for the location), referred to as the “element temperature,” tracks similar to the pan temperature for all experiments. An example of this can be seen in Figure 30. This temperature is an approximation of the air temperature near the center of the heating element. The maximum temperature observed during the normal cooking was 387.7 °C (729.9 °F) for experiment 6. The maximum temperature occurred immediately following the addition of the second batch of bacon. Presumably the maximum temperature was due to the empty pan and the added bacon cooled the pan. After normal cooking was complete, the temperature was less than the value seen when the batch was removed from the pan. The temperatures of the pan and element converge as the pre-flame condition was approached.

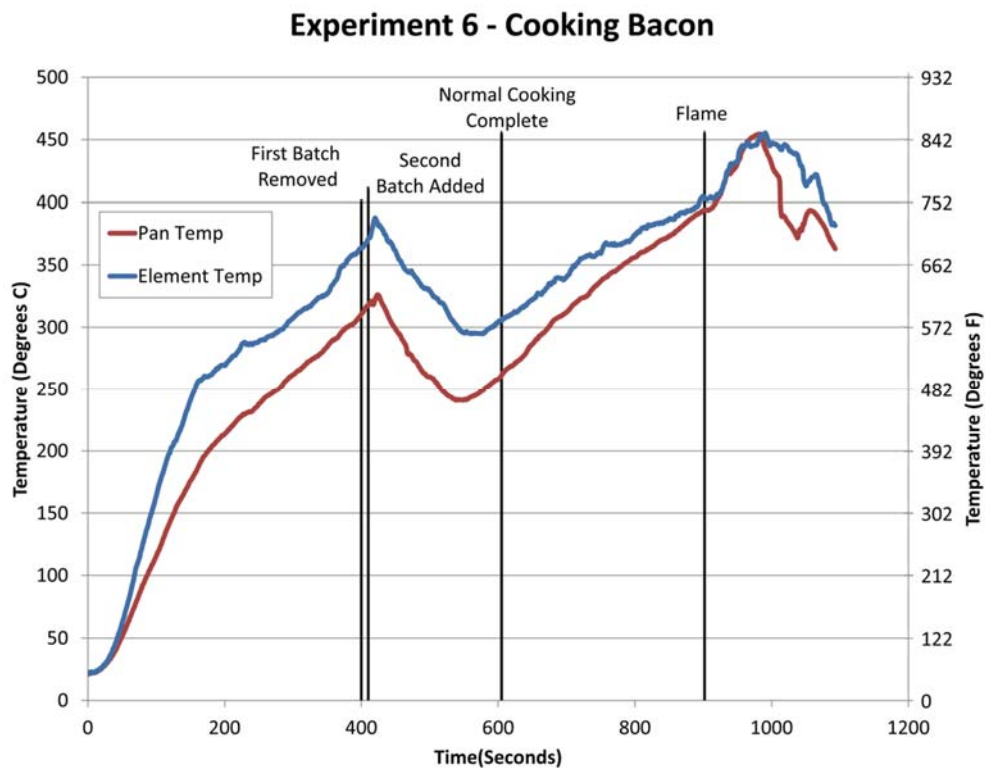


**Figure 30: Experiment 6 Pan & Element Temperature Graph**

A similar condition occurs in experiments 3 with the blackened fish, where once the fish is removed from the pan, both the element and pan temperature continue to rise until 30-60 seconds after the second batch is added to the pan and the temperature of both the pan and the element begin to decrease. The temperatures of the pan and element after the normal cooking completed are again lower than the peak seen during the empty pan. Experiment 3 was conducted as normal cooking thus no conclusion can be drawn between the pan and element temperature for an impending cooking fire.

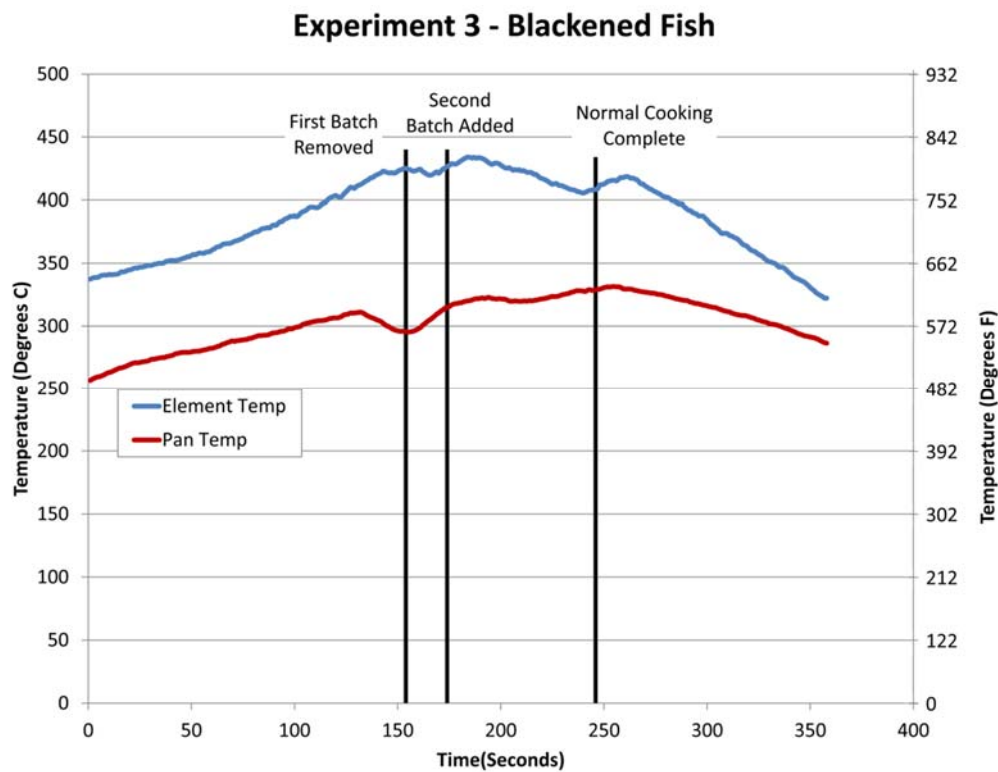


**Figure 31: Experiment 3 Pan and Element Temperature Graph**

Element temperature does provide some indication of an impending cooking fire as seen in Table 7 as the values for the pre-fire maxima exceed the values found in normal cooking for the majority of the experiments. The exceptions are experiment 6 with the elevated normal cooking

value due to the empty bacon pan and experiment 3 where the blackened fish was done at a higher pan temperature. In all the other cases, pre-fire maximum temperatures exceeded 450 °C (842 °F). Although there is some overlap in the range as indicated in Figure 32, the majority of the experiments show a strong distinction between the normal cooking and pre-fire stages, suggesting a thermocouple probe placed near the center of an electric element may serve as a precursor signal to an impending cooking fire. Further research is required to evaluate the effectiveness of a thermocouple positioned at the center of a gas burner to act as a precursor signal to an impending cooking fire.

**Table 7: Element Temperature Normal & Pre-Fire – All experiments**

	Normal Cooking	Pre-Fire
Experiment Number	Maximum Temperature °C (°F)	Maximum Temperature °C (°F)
1	N/A	514.60 (958.28)
2	247.31 (477.16)	N/A
3	434.01 (813.22)	N/A
4	Sensor Error	624.91 (1156.8)
5	358.05 (676.49)	N/A
6	387.66 (729.79)	392.52 (738.54)
7	N/A	614.11 (1137.40)
8	N/A	470.34 (878.61)
9	N/A	575.29 (1067.5)
10	352.89 (667.20)	481.03 (897.85)
11	N/A	53.92 (129.06)
Range	247.31 – 434.01 (477.16 – 813.22)	53.92 – 624.91 (129.06 – 1156.8)
Average	355.98	465.84

N/A – Not Applicable

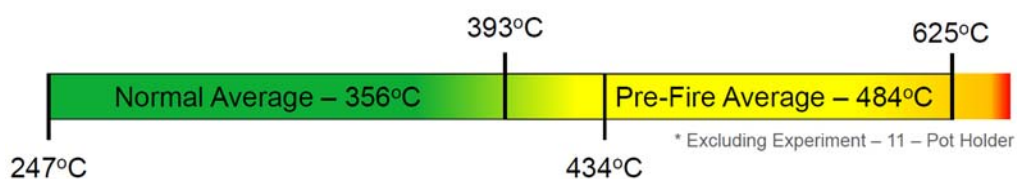


**Figure 32: Element Temperature Range – Normal Cooking and Pre-Fire**

A thermocouple placed at the center of an electric burner shows promise as an effective solution to monitor for an impending cooking fire. Unlike the pan temperature, the thermocouple would not need to be in contact with the pan and would have minimal if any effect on a user's cooking habits. Additional research and testing is recommended to evaluate the effect on boiling water and the flambé cooking style.

### Oil Temperature

Conducted for only experiment 10, peanut oil and French fries, the oil temperature would be a precursor signal to an impending autoignition of the oil in the pan, however due to the various ignition temperatures of cooking oils, the non-homogeneous temperature profile in the oil and the difficulty measuring the signal without causing significant interruption to the occupants' cooking practices, oil temperature would not be an desirable pre-cursor signal to cooking related fires.

### Particle Analyzer

The particle analyzer counted the number of smoke particles for 48 different size ranges (bins). The first 24 bins are measured by a condensation particle counter (CPC), the next 24 by light scattering. Calculations involve the 24 CPC bins less than 500 nm and the 19 light scattering bins greater than 500 nm (0.0197 mils). This allows for an evaluation of the particle size, particle density. In addition the data can be utilized to develop calculated values for ionization signal strength, scattering and obscuration.

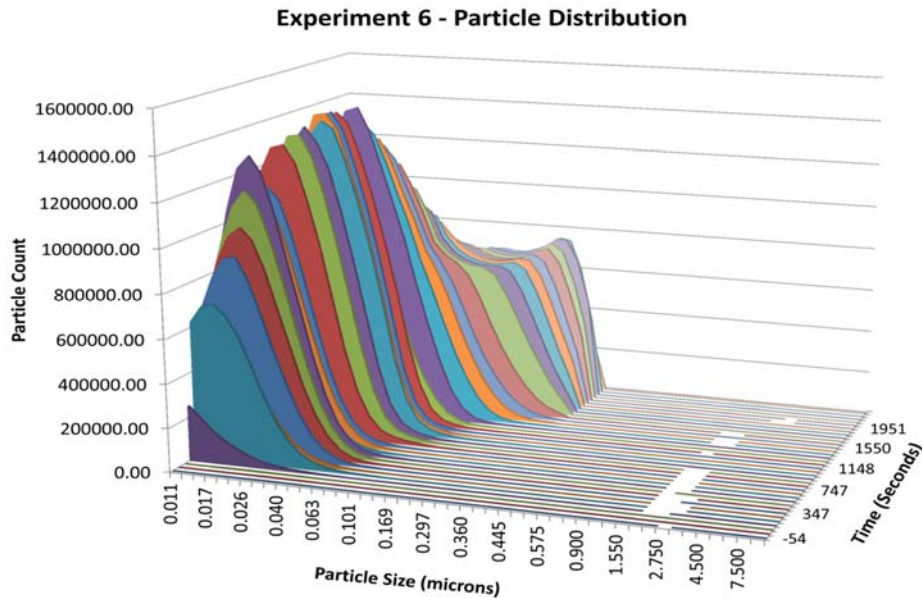


**Figure 33: Experiment 6 – Particle Size Distribution**

As an example, Figure 33 indicates the data recorded by the particle analyzer during experiment 6. The normal cooking period ended at 1,104 seconds and the particle size increased over the remainder of the experiment until ignition occurred at 2,232 seconds. The trend to larger particle size after normal cooking was complete is evident.

The data from the particle analyzer can be post processed to produce the average particle size in microns, the total number of particles per centimeter cubed, and a breakdown of visible and invisible particles.

The average particle diameter allows for an approximation of particle size. The maximum value of this particle size approximation during normal cooking and pre-fire conditions are included in Table 8. As shown in the table, the average particle size for the experiments where normal cooking occurred, increased from the normal cooking to the pre-fire stages. In the experiments

that transitioned from normal cooking to a pre-fire or hazardous condition stage, the particle size increased between the two stages. Experiment 4 was the outlier which saw a decrease in average size from the normal cooking to the pre-fire stage. This suggests to the potential for using particle size as a pre-cursor signal to an impending cooking fire.

**Table 8: Average Particle Size Normal & Pre-Fire – All Experiments**

	Normal Cooking	Pre-Fire
Experiment Number	Maximum Average Particle Diameter microns (mils)	Maximum Average Particle Diameter microns (mils)
1	N/A	0.1047 (0.0041)
2	0.1461 (0.0058)	N/A
3	0.1110 (0.0044)	N/A
4	0.1436 (0.0057)	0.1287 (0.0051)
5	0.1457 (0.0057)	N/A
6	0.1101	0.1918 (0.0076)
7	N/A	0.1170 (0.0046)
8	N/A	0.1648 (0.0065)
9	N/A	0.1141 (0.0045)
10	0.0606 (0.0024)	0.1544 (0.0061)
11	N/A	0.1887 (0.0074)
Range	0.0606 – 0.1461 (0.0024 – 0.0058)	0.1047 – 0.1918 (0.0041 – 0.0076)
Average	0.1195 (0.0047)	0.1455 (0.0057)

N/A – Not Applicable

The ranges of average particle size values for normal cooking as compared to pre-fire show an overlap which indicates the potential for nuisance situations to arise if particle size alone was used as a pre-cursor signal. The values for Experiment 2 – Browning Hamburger, Experiment 4 – Vegetables and Experiment 5 – Seared Steak for normal cooking exceeded the values recorded during the pre-fire period for several experiments indicating a reasonable threshold value does not exist. Although particle size shows some indication of being a precursor signal, the lack of consistency throughout the individual experiments coupled with the overlapping range would

make particle size a poor pre-cursor signal for impending fire. The number of particles per centimeter cubed will provide an approximation of the particle count density. As seen in Table 9 the maximum particle count density for all experiments does not vary greatly between the normal cooking and the pre-fire periods. For those experiments where normal cooking transitioned to pre-fire and fire stages the particle count density increases significantly. Normal cooking in experiment 3 – blackened fish and experiment 10 – French fries in peanut oil both illustrate a larger density of particle counts then seen in the pre-fire stages for all but experiment 9 – corn oil and experiment 10 – peanut oil and French fries.

**Table 9: Maximum Particle Density Normal & Pre-Fire – All Experiments**

	Normal Cooking	Pre-Fire
Experiment Number	Maximum Particle Count per cm <sup>3</sup> (per in <sup>3</sup> )	Maximum Particle Count per cm <sup>3</sup> (per in <sup>3</sup> )
1	N/A	1.520 x 10 <sup>6</sup> (2.491 x 10 <sup>7</sup> )
2	2.879 x 10 <sup>4</sup> (4.718 x 10 <sup>5</sup> )	N/A
3	1.091 x 10 <sup>7</sup> (1.788 x 10 <sup>8</sup> )	N/A
4	1.044 x 10 <sup>6</sup> (1.711 x 10 <sup>7</sup> )	4.195 x 10 <sup>6</sup> (6.874 x 10 <sup>7</sup> )
5	6.105 x 10 <sup>6</sup> (1.000 x 10 <sup>8</sup> )	N/A
6	6.001 x 10 <sup>6</sup> (9.834 x 10 <sup>7</sup> )	9.632 x 10 <sup>6</sup> (1.578 x 10 <sup>8</sup> )
7	N/A	6.707 x 10 <sup>6</sup> (1.099 x 10 <sup>8</sup> )
8	N/A	7.804 x 10 <sup>6</sup> (1.279 x 10 <sup>8</sup> )
9	N/A	1.026 x 10 <sup>7</sup> (1.681 x 10 <sup>8</sup> )
10	1.226 x 10 <sup>7</sup> (2.009 x 10 <sup>8</sup> )	1.060 x 10 <sup>7</sup> (1.737 x 10 <sup>8</sup> )
11	N/A	1.462 x 10 <sup>6</sup> (2.396 x 10 <sup>7</sup> )
Range	2.879 x 10 <sup>4</sup> – 1.226 x 10 <sup>7</sup> (4.718 x 10 <sup>5</sup> – 2.009 x 10 <sup>8</sup> )	1.462 x 10 <sup>6</sup> – 1.060 x 10 <sup>7</sup> (2.396 x 10 <sup>7</sup> – 1.737 x 10 <sup>8</sup> )
Average	6.522 x 10 <sup>6</sup> (1.069 x 10 <sup>8</sup> )	6.053 x 10 <sup>6</sup> (9.919 x 10 <sup>7</sup> )

N/A – Not Applicable

The overlapping ranges seen between normal fire and pre-fire along with no discernible difference between the values in fire and pre-fire stages as seen in Figure 34 would rule out particle count density as a pre-cursor for an impending cooking fire.

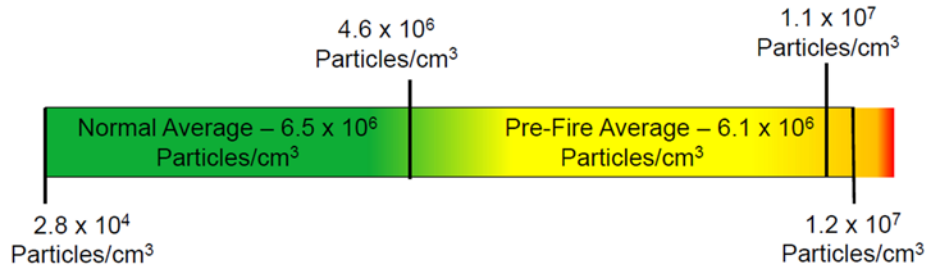


**Figure 34: Particle Density Range – Normal Cooking and Pre-Fire**

The evaluation of the calculated values of ionization signal strength, obscuration and scattering produce similar results to the particle density as they are derived from the raw data used to develop the particle count and density tables above. Although individual experiments show an increase in overlapping values between normal and pre-fire, the range of values overlap and would not serve as a consistent pre-cursor signal for impending cooking fires.

#### Oxygen Concentration



The oxygen concentration values during all experiments remained in the normal ranges found within common occupancies.

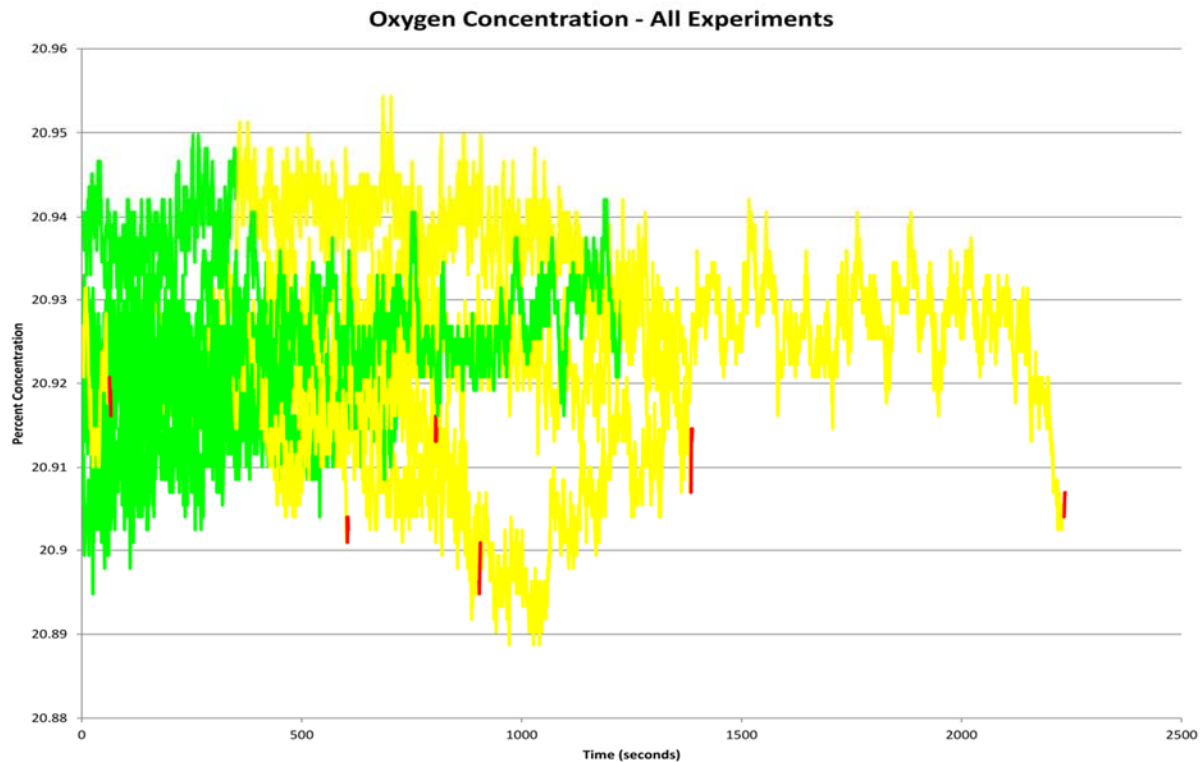
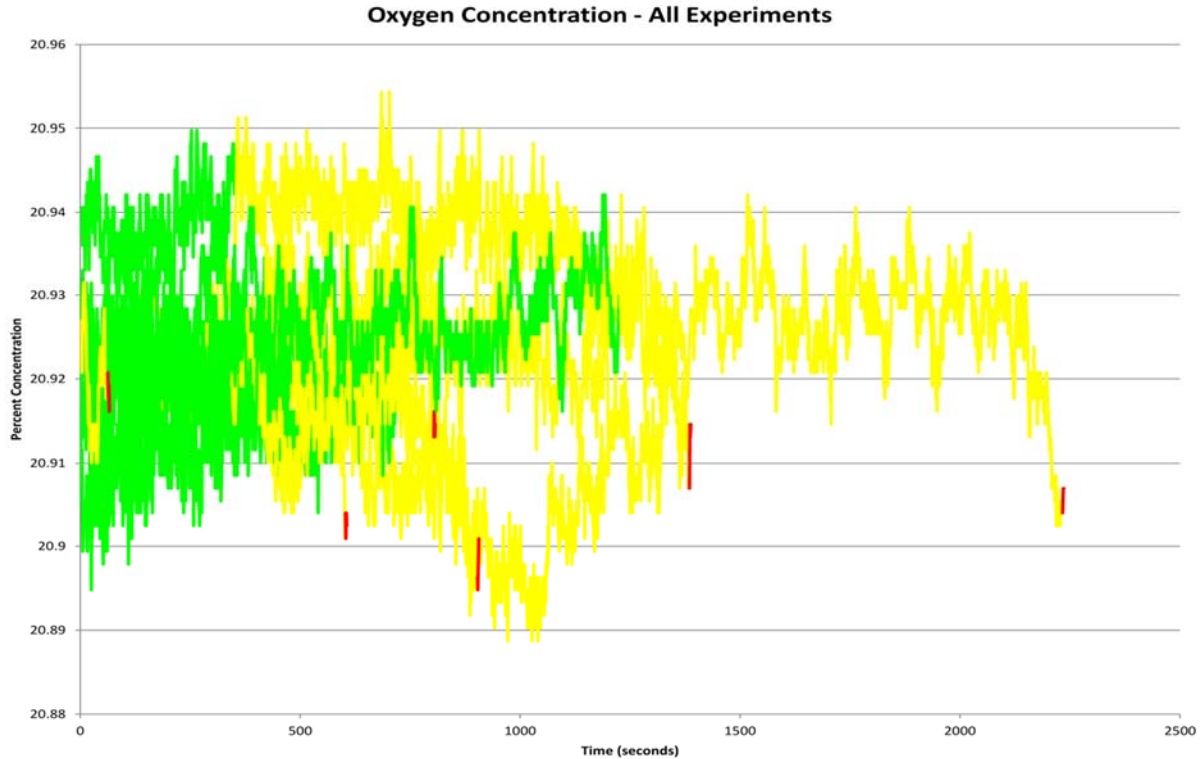


Figure 35 shows the oxygen concentration percentage varied between 20.89% volume and 20.95% volume for all experiments. The green values in the figure represent normal cooking, the yellow represent the pre-fire stage and the red represent the point of transition to flame. As depicted in Figure 35 the values do not vary between normal cooking and pre-fire, thus oxygen concentration would not provide an indication of impending cooking fire.



**Figure 35: Oxygen Concentration – All Experiments**

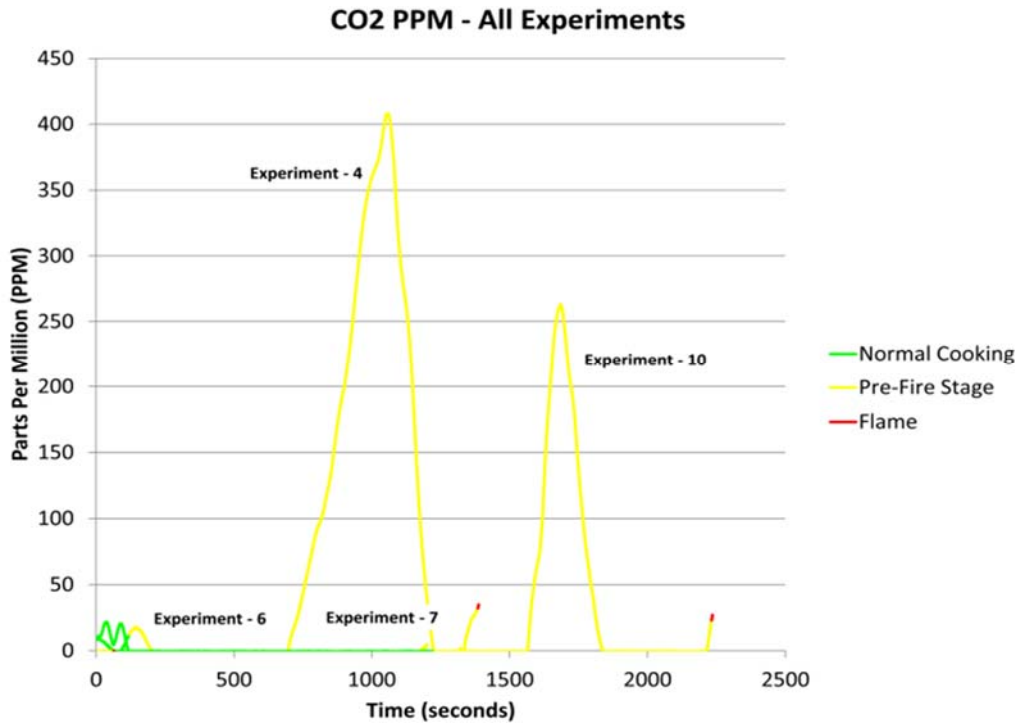
### Carbon Dioxide Concentration

Table 10 indicates the average CO<sub>2</sub> concentration recorded for the normal stage and pre-fire stage of each experiment along with the overall range of values for each stage and average over all experiments. Figure 36 illustrates the ranges of values over time for each experiment with the experiments with outlying values highlighted. Three experiments showed an increase in CO<sub>2</sub> concentration over ambient conditions. Experiment 4 – vegetables, experiment 7 – cooking oil, and experiment 10 – peanut oil and French fries all show an elevated value during pre-fire stages which is not detected during any of the normal cooking. Experiment 6 – bacon shows an increase in CO<sub>2</sub> however it does not increase above the normal cooking values shown in other experiments.

**Table 10: Maximum CO<sub>2</sub> ppm Normal Cooking & Pre-Fire – All Experiments**

	Normal Cooking	Pre-Fire
Experiment Number	Maximum CO <sub>2</sub> (ppm)	Maximum CO <sub>2</sub> (ppm)
1	N/A	0
2	0	N/A
3	0	N/A
4	0	408
5	0	N/A
6	22	0
7	N/A	16
8	N/A	0
9	N/A	0
10	0	242
11	N/A	0
Range	0 - 22	0 – 408
Average	3.3	53.3

N/A – Not Applicable



**Figure 36: Comparison CO<sub>2</sub> Percentage Concentration to CO<sub>2</sub> ppm for all experiments**

The use of CO<sub>2</sub> as a precursor signal is summarized further in Table 10 where the pre-fire signal is evaluated over the range developed for detection. In all the experiments with the exception of experiment 6 – bacon, the normal CO<sub>2</sub> concentration was 0 ppm, with a value of 22 ppm for the cooking of bacon. The CO<sub>2</sub> concentration increase for experiment 6 occurred during the first 2 minutes and 10 seconds when no interaction was occurring and the pan was warming. The CO<sub>2</sub> then dropped to 0 ppm and remained low, which may be attributed to the pan not being sufficiently cleaned between tests. Not all experiments show an increase in CO<sub>2</sub> during the pre-fire stage.

Although for some experiments CO<sub>2</sub> would provide a potential pre-cursor signal to an impending fire, the inconstant nature of the CO<sub>2</sub> values diminishes its effectiveness. Because the CO<sub>2</sub> was as low as zero in pre-fire conditions, there is no definable range for normal cooking that doesn't overlap with pre-fire conditions. As a consequence, pre-fire detection relying solely on CO<sub>2</sub> should be expected to be plagued by nuisance alarms. Hence CO<sub>2</sub> is not an effective pre-cursor signal to impending cooking fires.

#### Carbon Monoxide Concentration

Throughout all the experiments the values for CO remained at 0 ppm during normal cooking as noted in Table 11. The maximum values of CO for the pre-fire stage are also presented in Table 10. In all experiments, CO values increase during the pre-fire stage with the exception of experiment 9 – Corn Oil and experiment 11 – pot holder.

**Table 11: Maximum CO ppm Normal Cooking & Pre-Fire – All Experiments**

	Normal Cooking	Pre-Fire
Experiment Number	Maximum CO (ppm)	Maximum CO (ppm)
1	N/A	14
2	0	N/A
3	0	N/A
4	0	252
5	0	N/A
6	0	92
7	N/A	146
8	N/A	3
9	N/A	0
10	0	339
11	N/A	0
Range	0	0 – 339
Average	0	106

N/A – Not Applicable

Experiment 9 – Corn Oil does exhibit an increase in CO prior to ignition as illustrated in the partial graph of the CO concentration in Figure 38 however that increase is not within the identified pre-fire/action period. The CO concentration increases at 595 seconds or 8 seconds prior to the ignition of the oil.

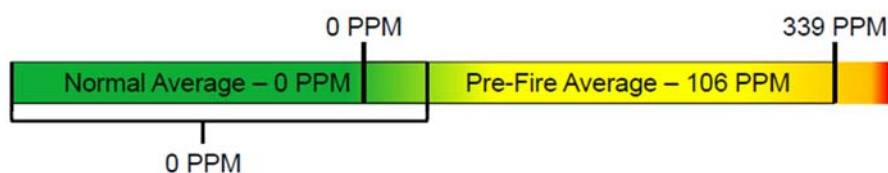


**Figure 37: Carbon Monoxide Concentration Range – Normal Cooking and Pre-Fire**

The range of normal cooking and pre-fire overlap for the experiments where the increase in CO did not occur within the pre-fire range (experiment 9 – corn oil and experiment 11 – pot holder), however all other experiments indicate a distinct increase in CO values from the normal cooking

to pre-fire stage. This can be seen graphically in Figure 37 where the pre-fire values of 0 ppm fall within the normal range. This would indicate limited interruption in normal cooking procedures due to false detection of a pre-fire indicator. The exception in experiment 9 would result in limited to no warning of the impending fire.

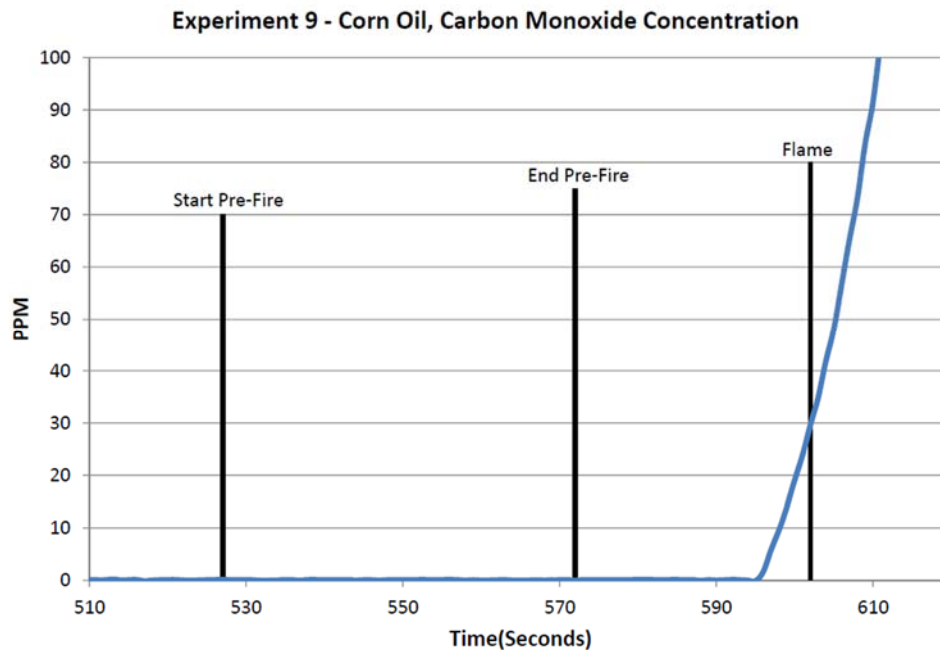


**Figure 38: Partial CO ppm Experiment 9 – Corn Oil**

### Optical Density

Obscuration measured at the three locations over the pan surface showed increased obscuration after normal cooking was completed. An example of this is illustrated for experiment 6 – Cooking Bacon in Figure 39. The increase indicated at about 400 seconds was due to the empty pan and the increase in particulate from burning the grease. At 535 seconds the beam was blocked by the turning of the bacon. A trend of increasing obscuration percentage is shown as the food content approaches autoignition.

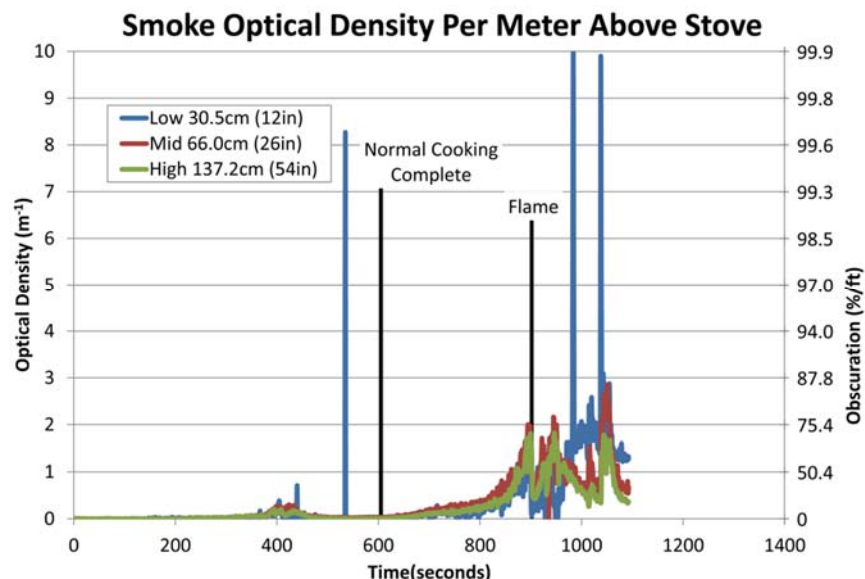


**Figure 39: Smoke Obscuration per Meter above Range – Experiment 6 – Corn Oil**

The maximum optical density recorded during the normal cooking and pre-fire stage at the middle sensor (located at the hood level) is presented in Table 12. A trend of increasing obscuration during the pre-fire stage with minimal to 0.301 OD/m (19.0 Obs  $\%/ft$ ) optical density during normal cooking is evident. The highest normal cooking obscuration was seen during experiment 3 – Blackened Fish, during experiment 5 – Seared Steak, and during experiment 6 – Bacon Cooking when the pan was empty between the two batches of bacon. The pre-fire stage for all experiments which transitioned to a flaming fire or unattended cooking resulted in optical density values exceeding 0.5 OD/m (29.5 Obs  $\%/ft$ ) with almost all reaching over 1.0 OD/m (50.3 Obs  $\%/ft$ ) at the hood level prior to the end of the pre-fire stage.

**Table 12: Maximum Obscuration during Normal Cooking & Pre-Fire – All Experiments**

	Normal Cooking	Pre-Fire
Experiment Number	Maximum Optical Density per Meter (Obscuration %/ft) – Hood Level	Maximum Optical Density per Meter (Obscuration %/ft) – Hood Level
1	N/A	1.638 (68.2)
2	0.035 (2.44)	N/A
3	0.251 (16.1)	N/A
4	0.092 (6.24)	1.16 (67.7)
5	0.271 (17.3)	N/A
6	0.301 (19.0)	1.07 (52.5)
7	N/A	3.09 (88.4)
8	N/A	1.54 (66.0)
9	N/A	1.56 (66.43)
10	0.04 (2.84)	Sensor Error
11	N/A	0.005 (0.374)
Range	0.035 (2.44) – 0.271 (17.3)	0.005 (0.374) – 3.09 (88.4)
Average	0.142 (9.44)	1.31 (60.1)

N/A

The data recorded for experiment 10 – peanut oil and French fries became corrupt after 1800 seconds. The optical density at the hood level prior to the data becoming corrupt is shown in Figure 40, where the optical density remains below the 0.5 OD/m (29.5 Obs %/ft) value of pre-fire until after the normal cooking was completed. Although data is not available for the pre-fire range between 91.5 seconds and 21.5 seconds prior to flaming fire, an increasing trend can be seen after normal cooking is complete.



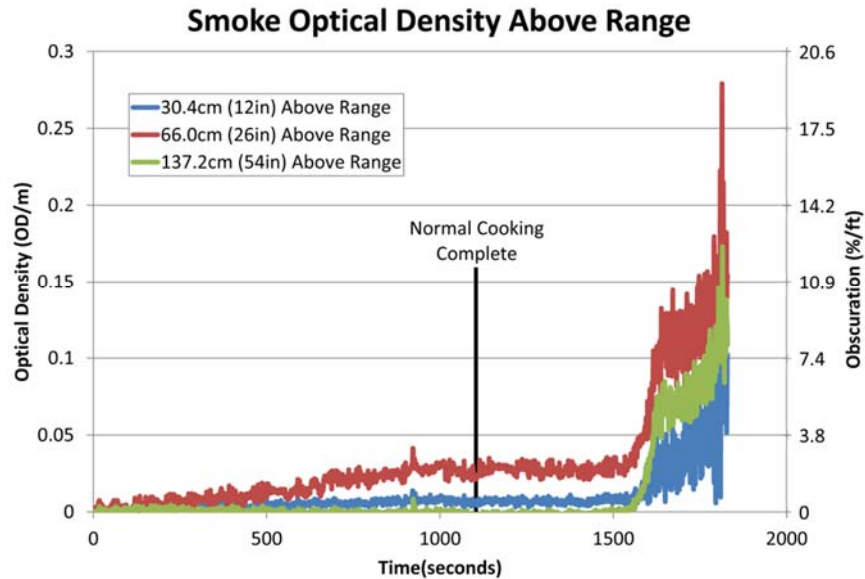


**Figure 40: Experiment 10 – Optical Density above Range**

The range of optical density values during normal cooking overlaps with the range of values in the pre-fire stage due to experiment 11 – Pot holder. This experiment transitioned to a flaming fire within 62 seconds which resulted in a pre-fire stage from between 0 seconds and 35.5 seconds, well prior to the optical density increase. When experiment 11 is excluded the range does not overlap as seen in Figure 41 where the minimum for the pre-fire range was 1.07 OD/m. As illustrated in Figure 42, this range was prior to any optical density increase however an increase does occur in excess of the 0.5 OD/m (29.5 Obs %/ft) value approximately 10 seconds before flaming fire.

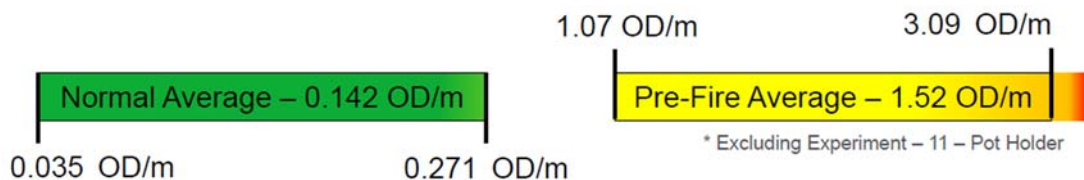


**Figure 41: Optical Density Range – Normal Cooking and Pre-Fire**

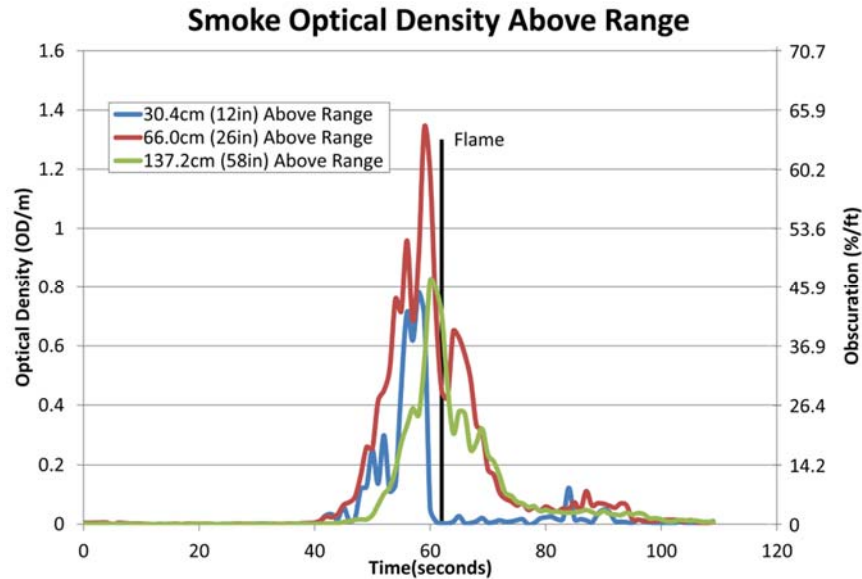


**Figure 42: Experiment 11 – Optical Density above Range**

As a precursor signal to impending cooking fires, obscuration provides an accurate means to identify the pre-fire stage. The sensor location at or within the hood would not impact the normal cooking procedures and the threshold value chosen has the potential to eliminate false predictions. Therefore obscuration is a plausible sensor for the prediction of impending cooking fires.

### Heat Flux

Heat flux was measured from the hood directed down toward the range. As seen in Table 13 the heat flux values for normal cooking ranged from just under 1.0 kW/m<sup>2</sup> to 2.33 kW/m<sup>2</sup> with the greatest values seen in the longer experiments. The overall heat flux increased from normal cooking to the pre-fire stage; however the ranges overlap significantly with the lowest pre-fire signal from experiment 4 – vegetables being seen in all but two of the normal cooking incidents for experiment 4 and experiment 2. Greater heat fluxes were seen in the longer duration experiments which may relate heat flux values more to cooking duration than the normal and

pre-fire stages. Heat flux does not appear to provide a reliable nuisance resistant sensor reading indicating an impending cooking fire.

**Table 13: Maximum Heat Flux for Normal and Pre-Fire Stage – All Experiments**

Experiment Number	Normal Cooking	Pre-Fire	Experiment Duration
	Maximum Heat Flux (kW/m <sup>2</sup> )	Maximum Heat Flux (kW/m <sup>2</sup> )	
1	N/A	3.01	19:45
2	0.92	N/A	6:35
3	1.92	N/A	4:44
4	0.81	1.95	22:03
5	1.17	N/A	11:56
6	2.33	1.79	15:02
7	N/A	3.31	23:04
8	N/A	2.55	13:23
9	N/A	1.95	10:02
10	2.28	Sensor Error	37:12
11	N/A	0.01	1:02
Range	0.92-2.33	1.79-3.31	
Average	1.57	2.03	

N/A – Not applicable

### Analog Smoke Alarm Signal

One ionization smoke alarm was located above the range and another on the ceiling of the kitchen. The analog signal used to identify a change in conditions by the manufacture was measured as a unit less relative value throughout all experiments. The average values recorded in each of the normal cooking and pre-fire stages of the experiments along with the activation status and overall average are located in Table 14. The range alarm activated in all but two of the experiments during normal cooking (experiment 2 – ground beef and experiment 4 – vegetables) indicating a high propensity for nuisance alarms. The analog signal however shows some tendency to indicate an impending cooking fire. The analog signal was at most 170 for the

normal cooking incidents and was above that for all of the pre-fire stages with the exception of experiment 6 – bacon. The pot holder in experiment 11 was not detected in the short, pre-fire window; however the alarm activated within 30 seconds of the flaming fire. The graphical representation of the range of signal values from the alarm is shown in Figure 43.

**Table 14: Range Analog Alarm Normal Cooking and Pre-Fire Stage – All Experiments**

Experiment Number	Normal Cooking	Pre-Fire
	Maximum Analog Ionization Signal	Maximum Analog Ionization Signal
1	N/A	198*
2	59	N/A
3	166*	N/A
4	98	188*
5	161*	N/A
6	170*	148*
7	N/A	198*
8	N/A	172*
9	N/A	222*
10	160*	219*
11	N/A	87**
Range	59 - 170	87 - 222
Average	135.6	179

\* Alarm activated

\*\*Alarm activated after transition to flaming fire.

N/A – Not Applicable

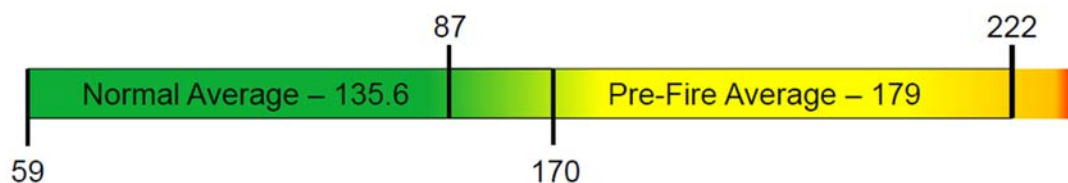


**Figure 43: Range of Alarm Signal from Ionization Alarm located on Ceiling above Pan – Normal and Pre-Fire Stages**

The ionization smoke alarm located 5.79 m (19 ft) from the range in the kitchen shows additional promise as a sensor for impending cooking fires. The analog signal values for this alarm reached a maximum value of 141 in the normal cooking scenarios and the minimum during pre-fire was 133 both occurring in experiment 6 – bacon, as indicated in Table 15. This was the only occurrence where the ionization analog signal did not increase from normal cooking to pre-fire conditions and no other normal cooking experiments show a value in excess of 140. The increase in the signal from the normal cooking stage to the pre-fire stage on average would indicate ionization analog signal may serve as a possible precursor signal to an impending cooking fire.

**Table 15: Kitchen Analog Alarm Normal Cooking and Pre-Fire Stage – All Experiments**

Experiment Number	Normal Cooking	Pre-Fire
	Maximum Analog Ionization Signal	Maximum Analog Ionization Signal
1	N/A	210*
2	76	N/A
3	135*	N/A
4	78	190*
5	136*	N/A
6	141*	133*
7	N/A	203*
8	N/A	150*
9	N/A	166*
10	114	196*
11	N/A	84**
Range	76 – 141	84 – 210
Average	113.3	166.5

\* Alarm activated

\*\*Alarm activated after transition to flaming fire.

N/A – Not Applicable

#### Analog CO Alarm Signal

The two CO alarms located above the range and 5.79 m (19 ft) away in the kitchen respectively did not activate during any of the experiments. The analog signals for both alarms are shown in

Table 16. Greater values for the analog signal were observed in those experiments where a layer of char formed on the bottom of the food in the pan including the normal cooking styles for searing steak in experiment 5 and browning ground beef in experiment 2. Also the normal cooking of vegetables in experiment 4 and bacon in experiment 4 provide high values where their respective pre-fire signals were lower in some instances and higher in others.

**Table 16: Range and Kitchen Analog CO Alarm Normal Cooking and Pre-Fire Stage – All Experiments**

Experiment Number	Range		Kitchen	
	Normal Cooking	Pre-Fire	Normal Cooking	Pre-Fire
	Maximum Analog CO Signal	Maximum Analog CO Signal	Maximum Analog CO Signal	Maximum Analog CO Signal
1	N/A	17	N/A	11
2	47	N/A	7	N/A
3	8	N/A	5	N/A
4	49	51	3	27
5	25	N/A	1	N/A
6	42	5	0	0
7	N/A	23	N/A	0
8	N/A	6	N/A	7
9	N/A	0	N/A	0
10	0	28	0	3
11	N/A	0	N/A	0
Range	0 – 49	0 – 51	0 – 7	0 – 27
Average	28.5	16.25	2.6	6

N/A – Not Applicable

Unlike the CO concentration from the gas analyzer shown in Table 11 , the alarms seem to register less of a difference between normal cooking and pre-fire conditions. This could be due to the location of the alarms being more remote from the source on the range. The experiments where flaming fires occurred did not register any change to the analog signal at the kitchen

alarm. The lack of a desirable signal difference between normal cooking and pre-fire conditions makes the analog signal from a CO alarm a poor precursor signal for impending cooking fires.

#### Commercial Ion/CO Alarm Analog Signal and Response

In Table 17, the maximum value for analog signal from the combination ion/co smoke sensor is shown for both normal cooking and pre-fire conditions. The alarms, located on opposite sides of the alarm array out in the kitchen, record similar signals within +/-13% for the normal cooking and +/- 23% for the pre-fire stage. The pre-fire values exceed the normal cooking values for all experiments with the exception of experiment 6 – frying bacon where the pre-fire signal was much less than the normal cooking values.

**Table 17: Commercially Available Ion/CO alarm Analog Signal Normal Cooking and Pre-Fire – All Experiments**

Experiment Number	Normal Cooking		Pre – Fire	
	Unit 1	Unit 2	Unit 1	Unit 2
	Maximum Analog Signal	Maximum Analog Signal	Maximum Analog Signal	Maximum Analog Signal
1	N/A	N/A	193	194
2	87	93	N/A	N/A
3	111	97	N/A	N/A
4	87	94	178	172
5	135	125	N/A	N/A
6	132	143	123	112
7	N/A	N/A	182	194
8	N/A	N/A	144	159
9	N/A	N/A	132	162
10	117	124	187	187
11	N/A	N/A	91	100
Range	87 – 143		100 - 194	
Average	112.1		156.9	

\* Alarm activated

\*\* Alarm Activated after Normal Cooking Complete

\*\*\* Alarm Activated after transition to flame.

N/A – Not Applicable

The alarms incorporated a pre-alarm condition. The alarm would internally process and verify the elevated signal prior to activating the audible alarm. The intent of this feature was to reduce nuisance or unwanted alarms. Figure 44 below shows the alarm performance in the various stages of the cooking experiments where the point indicates the activation time of the alarm. Unit 1 activated during normal cooking, however it also activated after the transition to a flaming fire. The second unit activated once during normal cooking in the same experiment that Unit 1 activated after flaming fire.

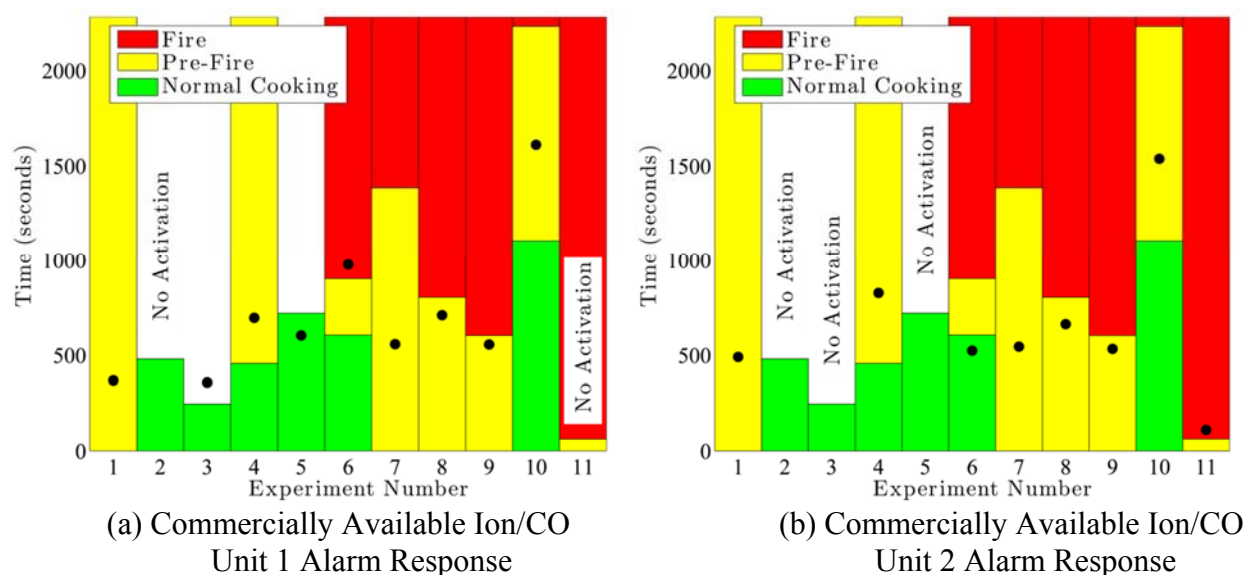


**Figure 44: Commercially Available Ion/CO Alarm Response – All Experiments**

The sensor technology utilized shows promise as a precursor signal to cooking fires however further research is required to verify the alarm point to determine the most effective threshold value to reduce nuisance alarms and provide the necessary action time to intervene and prevent the transition to a flaming fire.



## Smoke Alarm Array

The ionization, photoelectric, photo/ion, photo/co and advanced algorithm ionization smoke alarm technologies were placed on an alarm array to evaluate the effectiveness of the current devices and the nuisance alarms created. Figure 45 compares the ionization and photoelectric technologies. The alarms performed similarly with the exception of the oil experiments (experiment 8 through 10) where the photoelectric alarm activated much closer to the transition to fire and the ionization alarm activated as the oil was still in the early stages of being heated. Overall neither technology showed potential for serving as a precursor signal at their current threshold values as they activated during the normal cooking stage for the majority of the normal cooking experiments.

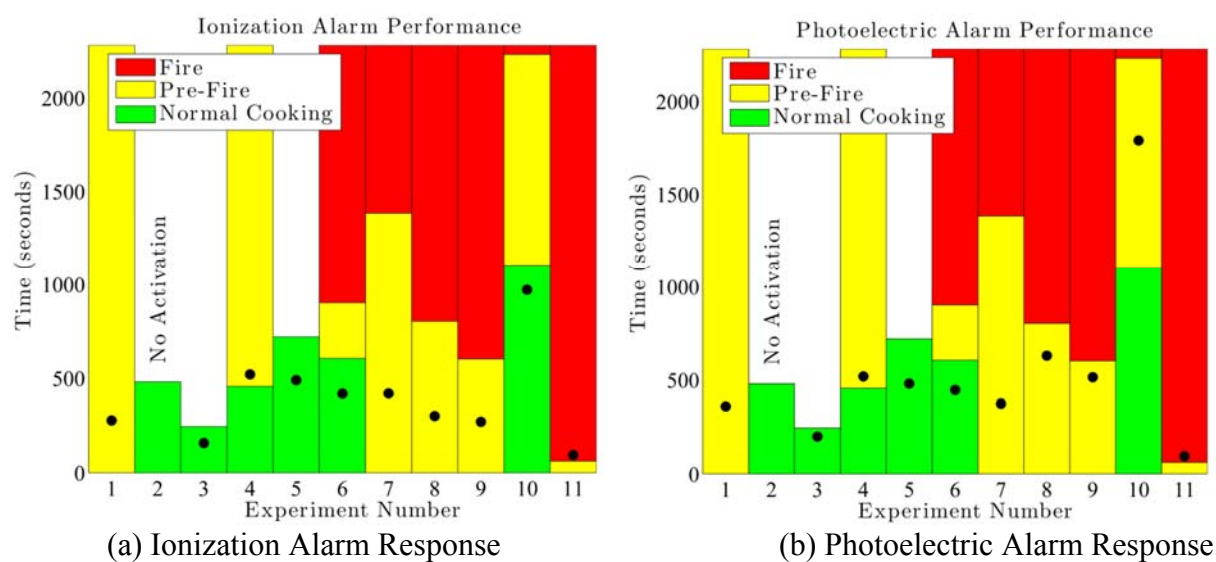


**Figure 45: Ionization vs. Photoelectric Alarm Response**

Comparing Figure 45 with Figure 46, the combination photo/ion unit appears to respond more similarly to the ionization unit than the photoelectric unit suggesting that the ionization sensor in the combination photo/ion unit seems to have driven the detection time. The one possible

exception is experiment 10 where the activation time of the combination photo/ion unit is between the individual ionization and photoelectric units. If the ionization signal drives the response time alone, the combination unit would not serve as a precursor signal at its current threshold values any better than an individual ionization sensor.

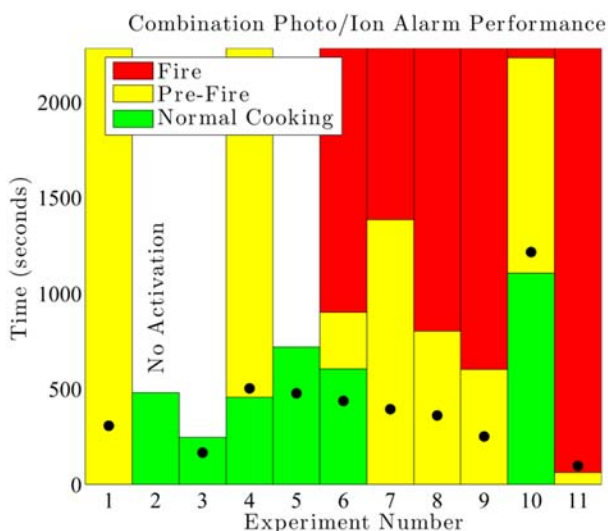


**Figure 46: Combination Photo/Ion Alarm Response**

The combination photoelectric and carbon monoxide alarm responded similar to the photoelectric alarm. Figure 47 shows the two alarms, where response occurred within the same time frame indicating the photoelectric sensor drove the activation time not the carbon monoxide signal. Thus the combination photoelectric and carbon monoxide alarm at their current alarm thresholds would not serve as a precursor signal to impending cooking fires any better than the stand-alone photoelectric alarm.

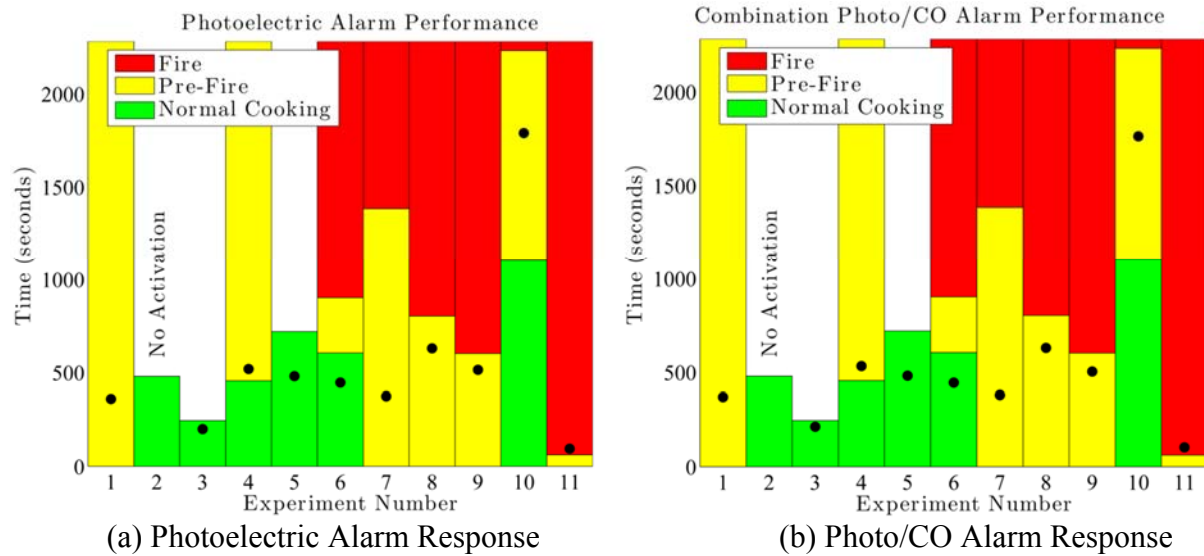


**Figure 47: Photoelectric and Photo/CO Alarm Comparison**

The advanced algorithm ionization sensor technology, developed by Universal Security Instruments, Inc., is designed to eliminate nuisance alarms from everyday cooking and other nuisance alarm sources such as cooking. The alarm performed well as a precursor signal to impending cooking related fires. As seen below in Figure 48, the alarm activated during the pre-fire period in all but two of the incidents, experiment 6 – bacon and experiment 11 – pot holder. The normal cooking periods saw no activation of the alarm nor did experiments with only normal cooking. The reaction time for the alarm, shown in Table 18, ranged from 842 seconds before transitioning to flaming fire to 48 seconds after transitioning to flaming fire. The reaction time falls within the 26.5 and 91.5 seconds pre-fire range identified for taking action to prevent the transition to fire.

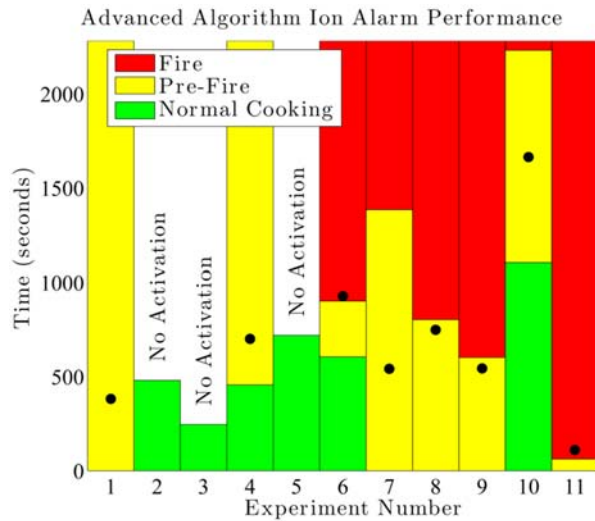


**Figure 48: Advanced Algorithm Ion Alarm Response Graph**

**Table 18: Advanced Algorithm Ion Alarm Response Time**

Experiment Number	Act Time (s)	Flame Time (s)	Reaction Time (s)
6	928	902	-20
7	542	1384	842
8	749	803	54
9	544	602	58
10	1664	2232	568
11	110	62	-48

Experiment 11 was not truly a cooking fire, thus the advanced algorithm ionization sensor only failed to alarm during the pre-fire stage for experiment 6 – bacon. In this experiment the alarm occurred 20 seconds after the transition to flaming fire. However, in contrast, experiment 7 which also involving cooking bacon in a different style, alarmed with over 14 minutes of time prior to transition which could be used to prevent transition from occurring. The propensity for this technology to alert occupants prior to transition to a flaming fire and its lack of nuisance alarms shows promise as a precursor signal to an impending cooking related fire. The technology should be evaluated further to confirm the results with a larger number and wider range of cooking related scenarios.

## Chapter 5: Analysis: Algorithm Development

### *5.1 Individual Sensor Algorithms*

Based on the results of the individual sensor analysis several sensors show promise to identify an impending cooking related fire. The most promising sensors identified were element temperature, carbon monoxide concentration, obscuration and ionization signal. To identify the most effective precursor signal an evaluation of the sensors are compared to determine their level of effectiveness. Each signal is evaluated for a potential threshold value based on a distribution of the normal cooking values recorded; each threshold is then tested against the entire data set to determine the response point and effectiveness.

#### Element Temperature

The element temperature thermocouple located at the center of the element shows promise as a precursor signal for an impending cooking related fire. The minimum value recorded aligns with the atmospheric temperature in the lab during testing at 21.84 °C (71.31 °F) and the maximum recorded during normal cooking was 434.01 °C (183.23 °F). Figure 49a shows a histogram of all data recorded during the normal stage of the experiments where one occurrence relates to one recorded value. The lower temperatures recorded were during heating of the element and do not represent a potentially hazardous situation. Figure 49b shows a histogram of the data distribution for the pre-fire stage with a minimum of 358 °C (676 °F) and a maximum of 625 °C (1157 °F).

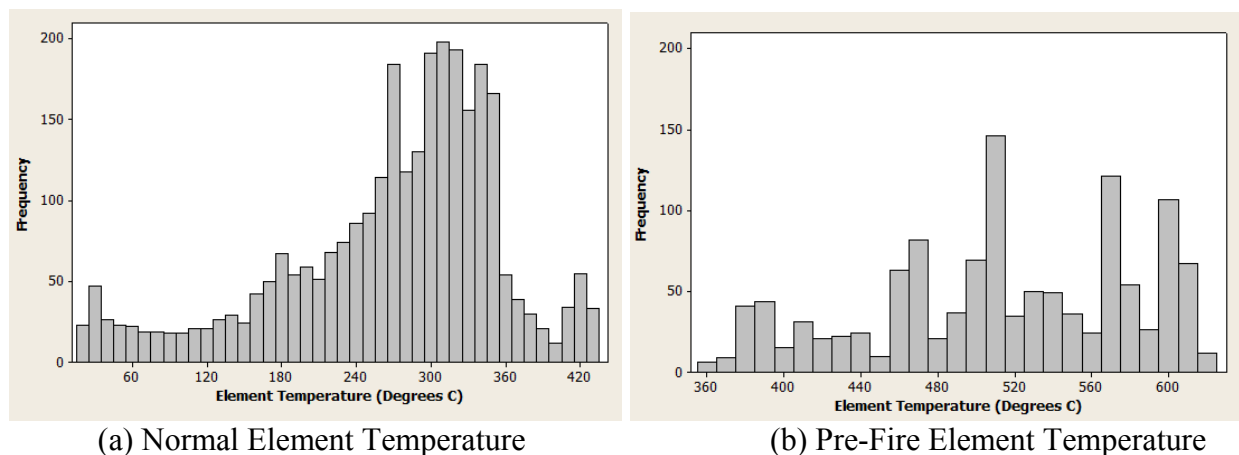


**Figure 49: Histogram of Element Temperature Distribution during Normal & Pre-Fire**

The normal element temperature data does not fit a normal distribution as determined by an Anderson-Darling test, thus to obtain a threshold value for use in a detection algorithm which would avoid nuisance alarms, 105% of the maximum of the normal value seen or 455 °C (851 °F) is used. This is 115°C higher than the threshold value suggested by the CPSC work of 340°C for a pan contact (Consumer Product Safety Commission, 1998) however the element sensor was not always in contact with the pan. The theoretical threshold was run through the experiments as an action point resulting in the detection of an impending fire as shown in Figure 50 and Table 19. The resulting data shows the identification of 4 of the 6 of the impending cooking fires, defined as those experiments where a fire occurs for an accuracy of 67% with reactions times which exceed the thermal inertia times recorded in the CPSC research. In addition, the algorithm identified correctly 6 of the 8 of the unattended cooking incidents, defined as the incidents which progressed from normal cooking to a hazardous condition. The algorithm was not successful in detecting the impending fire in experiment 6 – bacon as the theoretical activation was 89 seconds after flaming fire, nor was it successful in detecting the pot holder ignition on the burner in

experiment 11. No nuisance alarms occurred due to the selection of the threshold value being outside the data recorded during normal cooking.

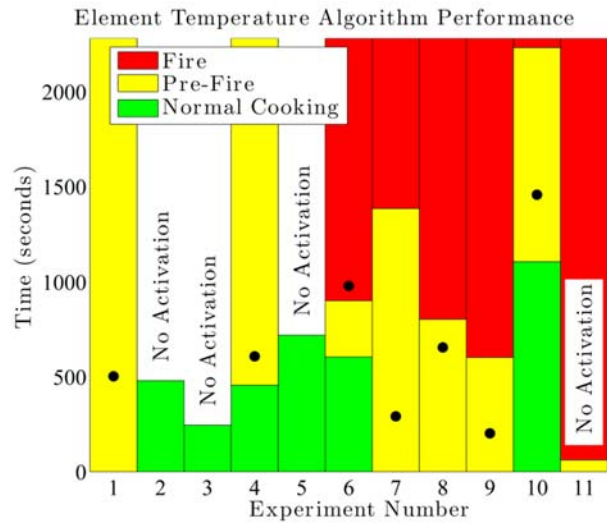


**Figure 50: Element Temperature Algorithm Response**

**Table 19: Element Temperature Algorithm Response Time**

Experiment Number	Act Time (s)	Flame Time (s)	Reaction Time (s)
1	521	N/A	N/A
2	No Act	N/A	N/A
3	No Act	N/A	N/A
4	615	N/A	N/A
5	No Act	N/A	N/A
6	991	902	-89
7	297	1384	1087
8	675	803	128
9	212	602	390
10	1498	2232	734
11	No Act	62	Missed Fire

N/A – Not Applicable

To determine the impact of the threshold selected, various thresholds from 435°C (815°F) to 475°C (887°F) were evaluated through a theoretical activation time and then compared to the normal cooking, pre-fire and fire times for each experiment. Figure 51 illustrates the results.

Varying the theoretical activation threshold for the element temperature will vary the activation time significantly for some experiments, however, the theoretical activation time remains in the same region of the experiment. The statistically obtained value of 455°C (851°F), provides the greatest reaction time while not interfering with normal cooking processes.

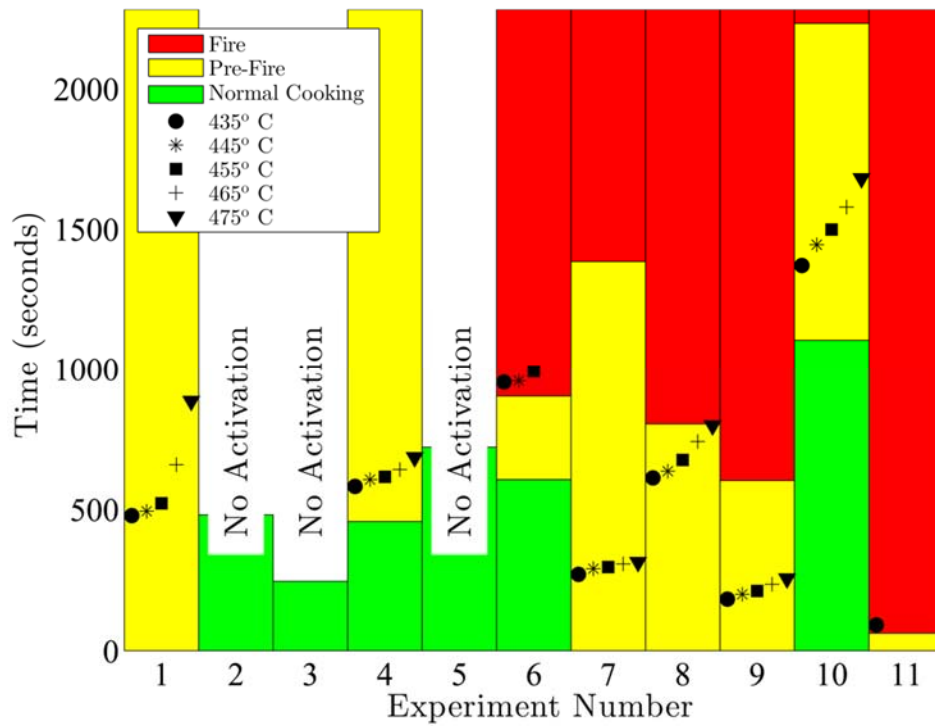


**Figure 51: Element Temperature Threshold Analysis**

Additional work is required to verify the finding above on other possible cooking scenarios.

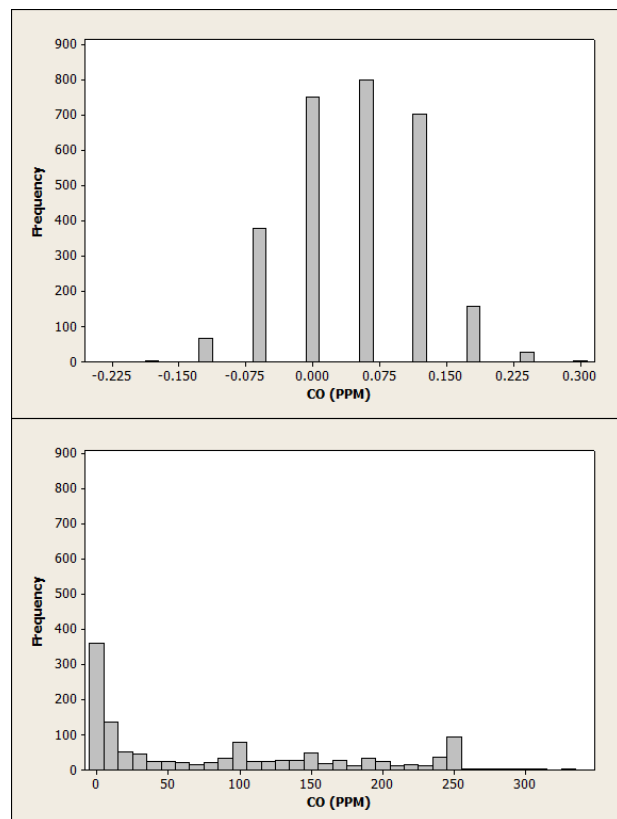
However based on the data from this set of experiments, air temperature at the center of the cooking element on an electric range appears effective in detecting impending cooking related fires with a reaction time capable of either human interaction or automatic shutdown of the cooking appliance.

### Carbon Monoxide Concentration

Carbon monoxide concentration has been tested and shows significant promise as a precursor signal for oil fires commonly seen during residential cooking in India (Ansari, et al., 2010). The data distribution for carbon monoxide during the normal cooking stage is shown in Figure 52. Values did not exceed 1 ppm during any of the normal cooking incidents; however the pre-fire stage shows an increase in carbon monoxide concentration detected. The sensitivity of the CO



meter was  $\pm 1\%$  in the initial range from 0 – 200 ppm or 2 ppm. A threshold value of 5 ppm was utilized to ensure the threshold was outside the error range of the meter.



(a) Normal CO ppm Data

Experiment Number	Act Time (s)	Flame Time (s)	Reaction Time (s)
1	78	N/A	N/A
2	No Act	N/A	N/A
3	No Act	N/A	N/A
4	508	N/A	N/A
5	No Act	N/A	N/A
6	846	902	56
7	1275	1384	109
8	777	803	26
9	597	602	5
10	1501	2232	731
11	81	62	-19

(b) Pre-Fire CO ppm Data

**Figure 52: CO ppm Data Distribution Normal& Pre-Fire**

The experimental data was analyzed against the threshold value of 5 ppm to develop Figure 53 and Table 20. The chosen threshold value eliminated nuisance alarms, however the threshold CO concentration is not developed until just prior to transition to a flaming fire. Five of the 6, or 83%, of the impending cooking fires were identified, with experiment 11 – potholder only being identified after transition to a flaming fire. The reaction time varied from the largest period of 731 seconds in experiment 10 – peanut oil and French fries to the shortest reaction times occurring for experiment 8 and experiment 9 with corn oil at 26 and 6 seconds

respectively. Experiment 11 – pot holder transitioned to a flaming fire before the theoretical detection time, however it would have been detected 19 seconds after transition to a flaming fire.

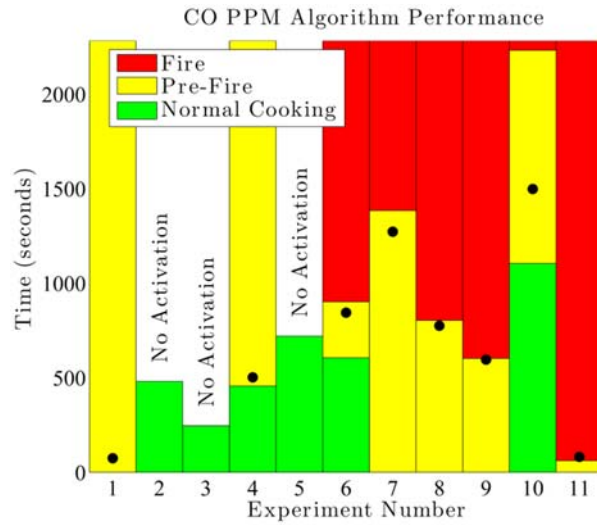


**Figure 53: CO Algorithm Response**

**Table 20: CO Algorithm Response Time**

Experiment Number	Act Time (s)	Flame Time (s)	Reaction Time (s)
1	78	N/A	N/A
2	No Act	N/A	N/A
3	No Act	N/A	N/A
4	508	N/A	N/A
5	No Act	N/A	N/A
6	846	902	56
7	1275	1384	109
8	777	803	26
9	597	602	5
10	1501	2232	731
11	81	62	-19

The response time for the statistically determined threshold 5 ppm was tested for effectiveness against other potential values to evaluate the reaction time provided and the phase of cooking fire which was detected. Values between 1 ppm and 9 ppm were evaluated as potential thresholds for all 11 experiments. As seen in Figure 54 the activation time does not vary with a variation in CO concentration. In each of the experiments when CO was detected by the gas analyzer the concentration increased rapidly in a matter of seconds. In an order to maintain the limited reaction time the values of 5 ppm was continued for the remainder of the evaluation of CO concentration in both signal and multi sensor analysis.

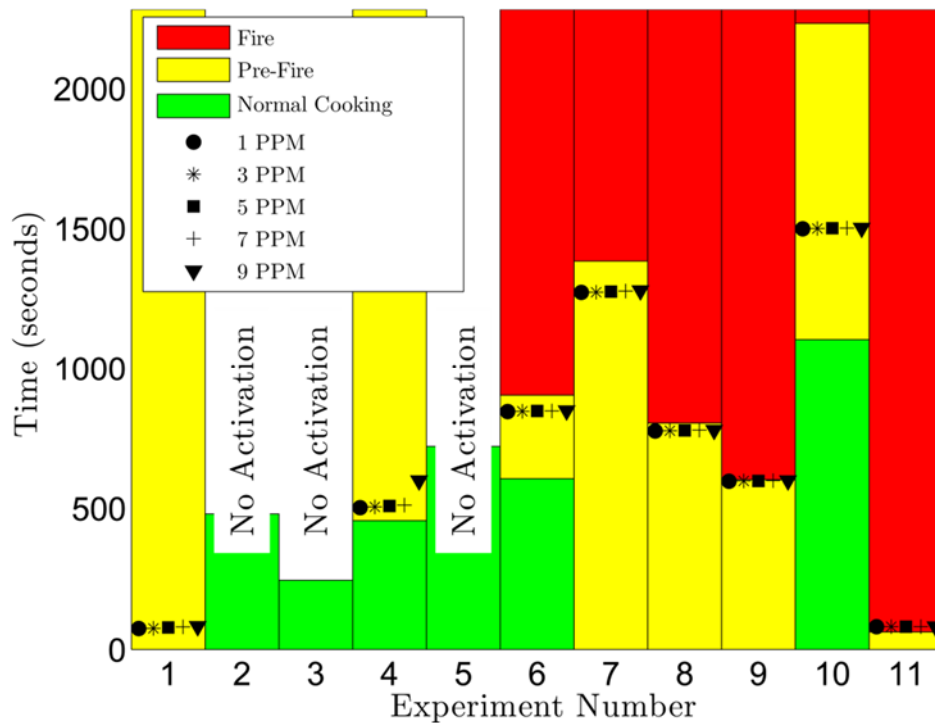


**Figure 54: CO ppm Multi Threshold Analysis**

Additional work is required to confirm the threshold for CO concentration identified here applies to other possible cooking scenarios. However based on the data CO concentration appears to give some indication of impending cooking related fires. The reaction time was shorter than the identified action period in 2 of the 6 of experiments which transitioned to fire suggesting sufficient notification may not be provided by CO concentration alone for an impending cooking related fire.

#### Optical Density Above Range

The data distribution of optical density recorded at the hood level during normal cooking is shown in Figure 55(a). The values remained at or near zero during all of the normal cooking stages. Figure 30 showing the maximum value recorded during each of the individual normal cooking for all experiments indicates a maximum of 0.271 OD/m occurred in experiment 6 – bacon. To remain above the normal cooking values and remain constant with industry standard

optical density thresholds, a value of 0.5 OD/m was chosen for the theoretical detection point.

The pre-fire data distribution of obscuration shown in Figure 55(b) encompasses the theoretical threshold values in the lower quarter of the data.

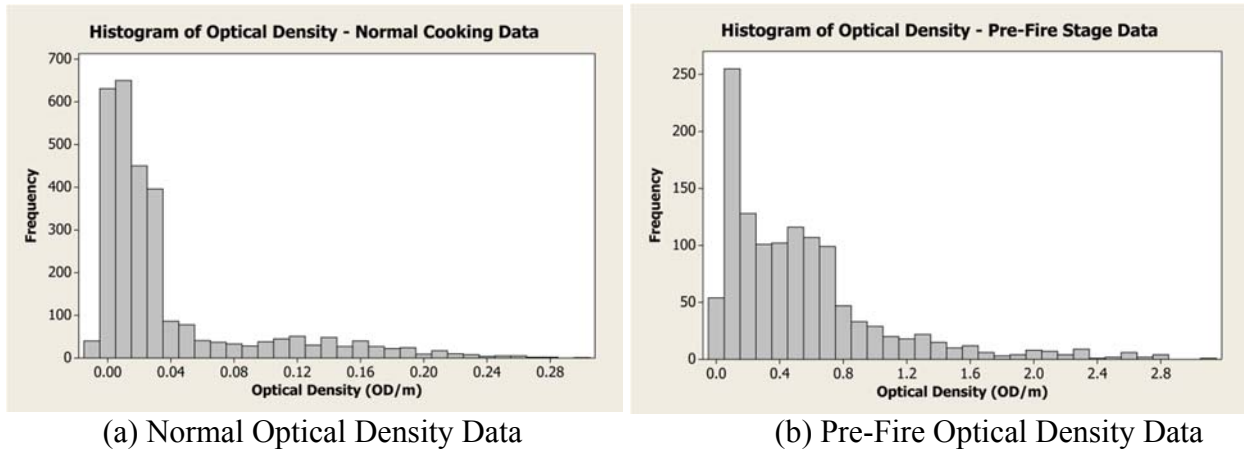


**Figure 55: Optical Density Data Distribution Normal & Pre-Fire**

The experimental data was analyzed against the theoretical maximum chosen as shown in Figure 56 where the impending cooking fire was predicted in five of the 6 (83%) fires correctly. A data collection failure occurred for the sensor in experiment 10 – peanut oil & French fries preventing a full analysis for this experiment. However an increase in optical density occurred after normal cooking, Figure 40, prior to the data collection failure. Extrapolating the increasing trend suggests the optical density would have exceeded the theoretical threshold prior to flaming fire resulting in the detection of the impending cooking related fire.

The theoretical threshold chosen excluded normal values and was capable of identifying the impending fire within the action time for 4 of the 6 impending cooking fires with the exceptions being experiment 10 – peanut oil and French fries as discussed above and experiment 11 – pot holder. In addition the algorithm was capable of predicting the unattended cooking which

occurred in experiment 1 – ground beef and experiment 4 – vegetables with an overall success rate of 8 out of 8 or 100%.

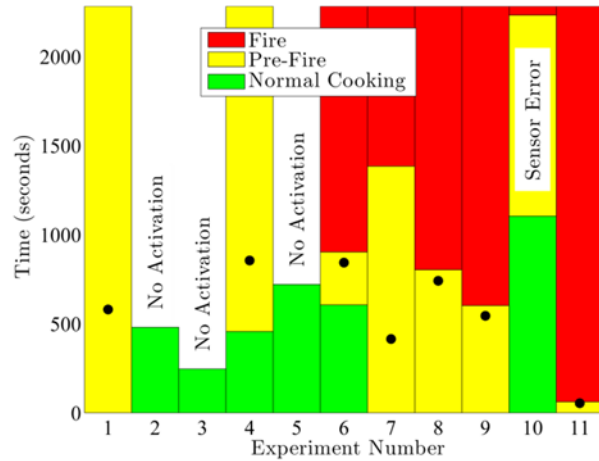


**Figure 56: Optical Density Algorithm Response**

**Table 21: Optical Density Algorithm Response Time**

Experiment Number	Act Time (s)	Flame Time (s)	Reaction Time (s)
1	580	N/A	N/A
2	No Act	N/A	N/A
3	No Act	N/A	N/A
4	855	N/A	N/A
5	No Act	N/A	N/A
6	843	902	59
7	414	1384	970
8	741	803	62
9	544	602	58
10	Error	2232	N/A
11	54	62	8

N/A – Not Applicable

The threshold of 0.5 OD/m was tested for effectiveness against other potential values to evaluate the reaction time provided and the phase of cooking fire which was detected. Values between 0.3 OD/m to 0.7 OD/m were evaluated as potential thresholds for all 11 experiments. As seen in Figure 57 the activation time varies slightly with a variation in the selected optical density threshold. In order to maintain a theoretical threshold outside the values of normal cooking, the 0.50 OD/m was maintained through the additional single sensor and multi sensor analysis.

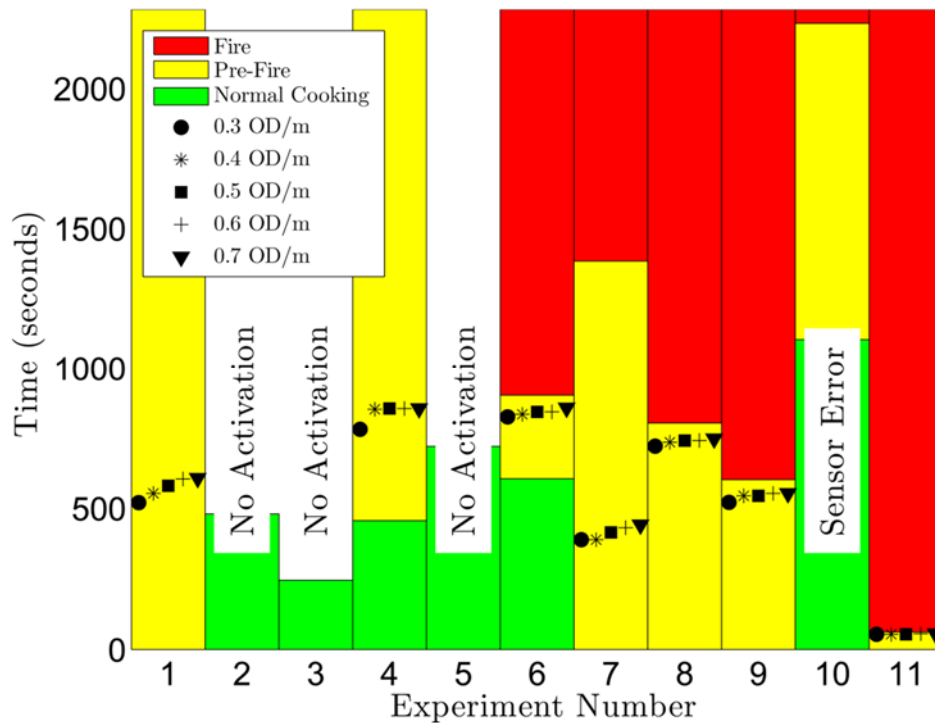


**Figure 57: Optical Density Threshold Analysis**

Optical density appears to be a strong pre-cursor signal to an impending cooking related fire at 0.5 OD/m which provided adequate reaction time for either human interaction or automatic shutdown of the cooking appliance. However additional work is required to verify the above findings on other possible cooking scenarios.

### Ionization Signal

The Ionization analog signal, is the monitored output from the ionization alarm. This value is used by the manufacturer's to identify a change in conditions and a threshold is set to coincide with activation. To establish a baseline in identifying an algorithm for this signal the manufactures threshold was identified for the particular alarm utilized. Based on the activations during experiments 1 and 3-11 the analog signal ranged from 111 to 146 when the alarm activated. A histogram of the analog signal at time of activation is shown in Figure 58 with a statistical normal curve fit to the data. The Anderson-Darling test was performed on the data and

results plotted in Figure 59 indicating P-Value exceeding 0.5 verifying the data set tends toward a normal distribution of 125. Thus the particular alarm utilized would have an average activation threshold of an average of 125. This factory threshold alarm value caused nuisance alarms in 80% of the normal cooking incidents as shown in Table 14 and falls inside normal value data distribution in Figure 61(a).

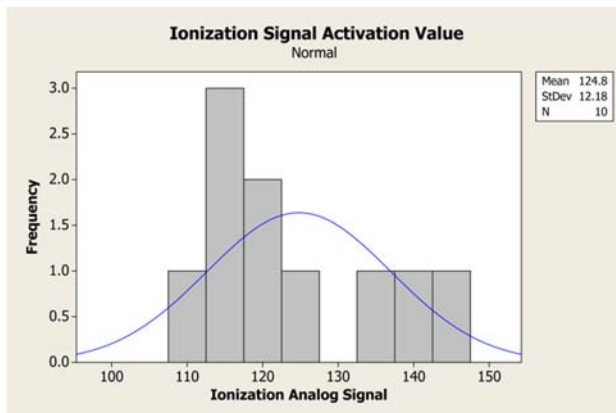


**Figure 58: Ionization Signal Activation Data Probability Plot**

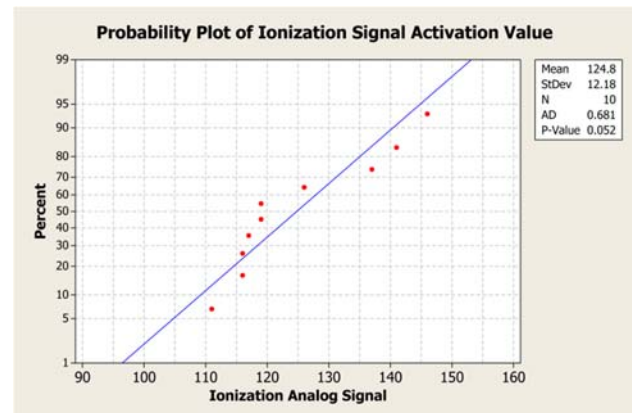


**Figure 59: Ionization Signal Activation Data Distribution**

For the purpose of this analysis a new threshold value for use in the algorithm was established. A histogram of the normal ionization analog signal is shown in Figure 61 where the data fell into two sections. This data was checked for normalcy using the Anderson-Darling method with the results plotted in Figure 60 which indicates the data does not fit a normal distribution, however there is a tendency toward normal distribution from the signal value of 50 to the signal value of 150 which incorporates 89% of the data or 2581 of the recorded 2885 values.

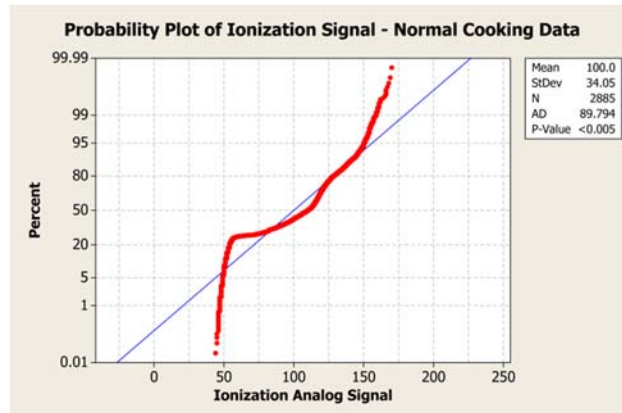


**Figure 60: Probability Plot of Ionization Signal – Normal Cooking Data**

To develop a threshold value, the data is treated as a normal distribution utilizing two standard deviations from the mean to assign a threshold value of 168 which falls within the normal data distribution however is greater than 2882 of the 2885 values. The value of 168 is within the pre-fire data distribution in Figure 61(b) which could potentially identify impending cooking fires.

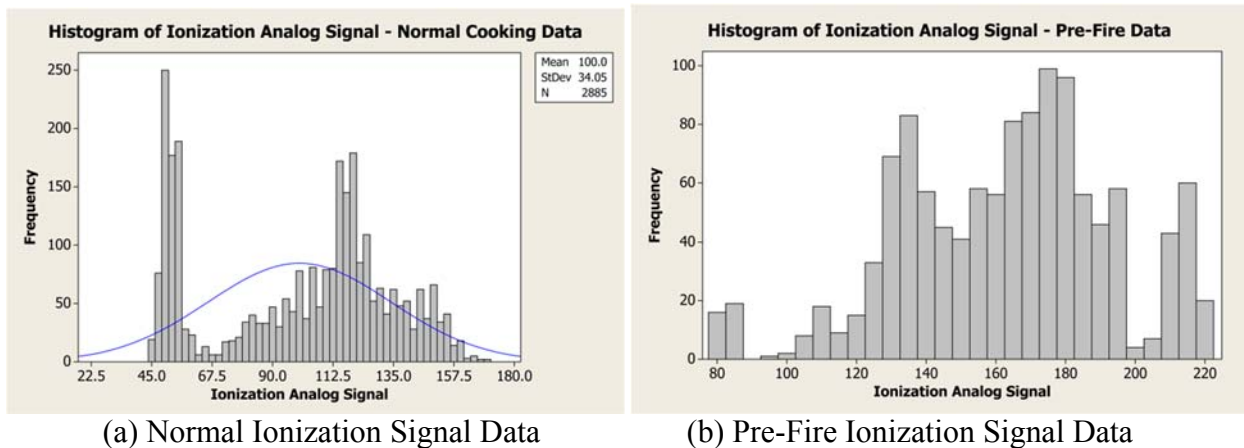


**Figure 61: Ionization Signal Data Distribution Normal & Pre-Fire**

The experimental data was analyzed against the theoretical maximum chosen as shown in Figure 62 where as expected experiment 6 – bacon resulted in a nuisance alarm as it the threshold chosen fell within the normal cooking data. However, 4 of the 6 or 67% of the impending fires were identified correctly. The unattended cooking incidents were also identified for 6 of the 8 or



75% of the hazardous conditions. No nuisance alarms occurred in the 3 normal cooking experiments thus the overall success rate was 8 of 10 or 80%. In the four experiments where the impending fire was correctly identified the reaction time exceeded the action time for three of the four and was within the action time for the fourth.

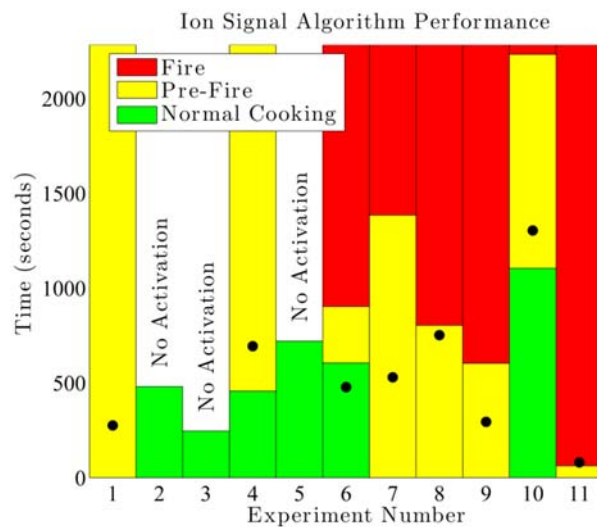


**Figure 62: Ionization Signal Algorithm Performance**

**Table 22: Ionization Signal Algorithm Response Time**

Experiment Number	Act Time (s)	Flame Time (s)	Reaction Time (s)
1	275	N/A	N/A
2	No Act	N/A	N/A
3	No Act	N/A	N/A
4	693	N/A	N/A
5	No Act	N/A	N/A
6	477	902	425
7	529	1384	855
8	751	803	52
9	294	602	308
10	1303	2232	929
11	80	62	-18

N/A – Not Applicable

The response time for the statistically determined threshold of 168 was tested for effectiveness against other potential values to evaluate the reaction time provided and the phase of cooking fire which was detected. Values between 148 and 188 were evaluated as potential thresholds for all 11 experiments, which are all still above the estimated manufacturer's threshold of 125 and the maximum alarm activation value of 146. As seen in Figure 63, the activation time varies significantly with a variation in the sensor threshold utilized. This variation is so significant that in some cases the activation would have been during normal cooking and others in the fire period. The statistically determined value of 168 will be utilized going forward as it provides the

most consistent activation during the pre-fire period without impacting normal cooking and allowing the greatest reaction time.

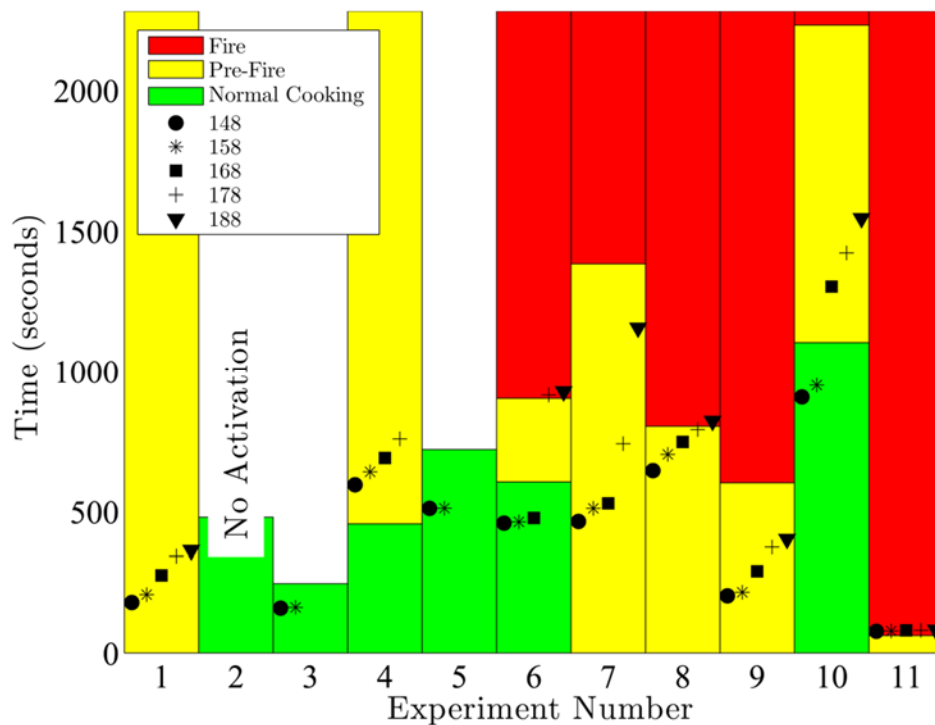


**Figure 63: Ionization Analog Signal Threshold Analysis**

The theoretical activation during Experiment 11 – pot holder was outside the reaction range and activation only occurs after transitioning to flaming fire. This is consistent with all other ionization alarm responses at other locations in the test enclosure, which all occurred after transition to flaming fire. Figure 64 shows the response of all ionization alarms during experiment 11 – pot holder. The alarms all responded after flaming fire occurred at 62 seconds and the delay resulting from increasing the alarm threshold for the range alarm would have theoretically only been 4 seconds.

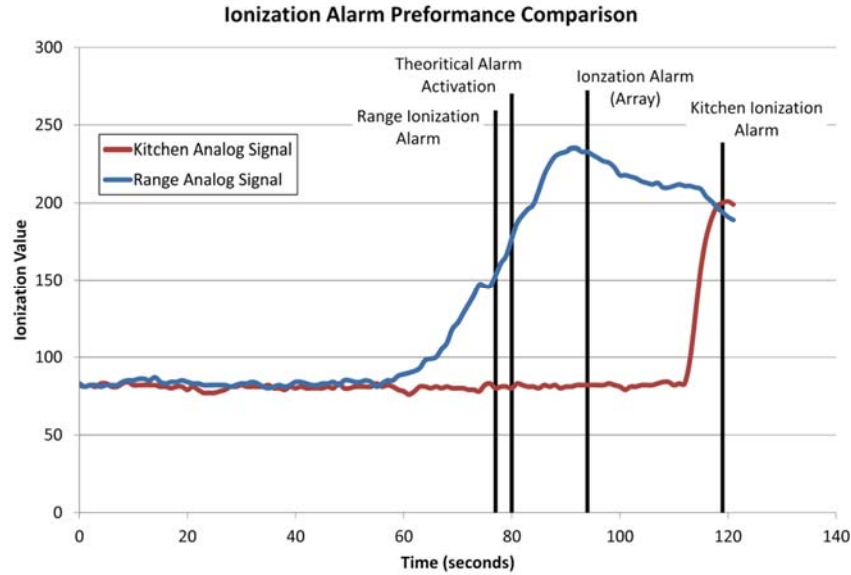


**Figure 64: Experiment 11 Ionization Alarm Performance Comparison**

Additional work is required to verify the above finding for other possible cooking scenarios; however, based on the data, increasing the threshold value of the analog ionization alarm appears to be a strong pre-cursor signal to an impending cooking related fire while providing sufficient reaction time for either human interaction or automatic shutdown of the cooking appliance.

## 5.2 Multi-Sensor Algorithms

The results from the individual sensors indicate a range of reaction times for the different food types and cooking styles. Optical density performed the most effectively in identifying the impending fires however ionization analog signal and element temperature provided a greater reaction time in 5 of the 6 (83%) of the incidents. Theoretically the ionization analog signal produced one nuisance alarm and the element temperature was not successful in predicting two of the six impending fires. These results suggest the inclusion of multiple sensors with an

intelligent algorithm may provide the greatest reaction time while preserving the ability to detect impending cooking fires while avoiding nuisance alarms.

Utilizing the threshold values for element temperature, ionization analog signal, and optical density element established during the evaluation of the individual sensor, in conjunction with an advanced algorithm, it is possible to maximize the theoretical reaction time. The algorithm identifies where any one of the three threshold values is exceeded during each experiment as indicated in the Figure 65.

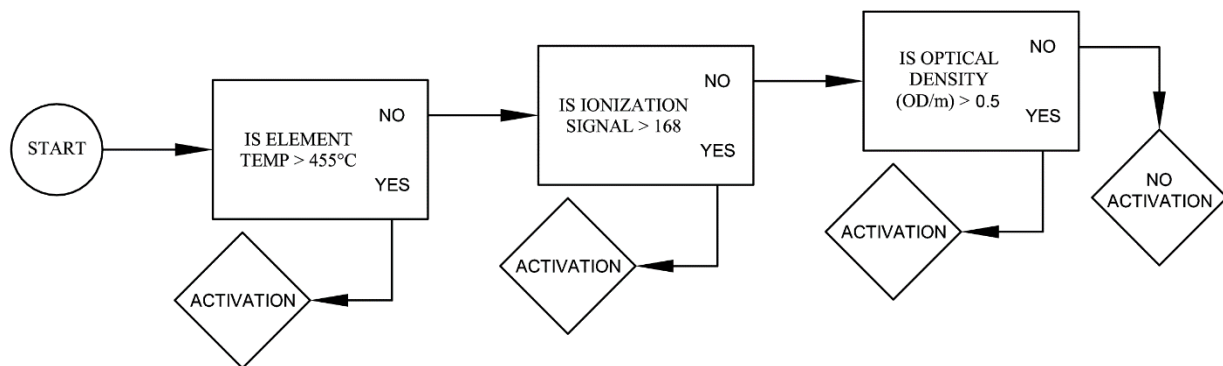


**Figure 65: Algorithm Logistical Flow Chart**

Through the use of the intelligent algorithm it was possible to identify 5 of 6 (83%) of the impending cooking fires correctly and 7 of 8 (88%) of the hazardous conditions. One false positive occurred for the impending cooking fire in experiment 6 however no false positives occurred for the hazardous conditions. As compared to the individual sensors the algorithm detected the pre-fire condition and limited nuisance alarms 16% more effectively than the element temperature, 33% more effectively than the CO concentration, 16% more effectively than the ionization analog signal but 17% less effectively than the optical density due to the

nuisance alarm. It was 13% more effective than the element temperature, 26% more effective than the CO concentration, 12% less effective than the optical density due to the additional nuisance alarm and 13% more effective than the ionization analog signal for detecting the hazardous condition.

**Table 23: Sensor Performance Comparison – Single Sensor vs. Multi-Sensor**

Experiment Number	Activation Time (s)				
	Element Temperature	Ionization Analog Signal	Optical Density	Algorithm	Simplified Algorithm
1	521	275	492	275	492
2	No Activation	No Activation	No Activation	No Activation	No Activation
3	No Activation	No Activation	No Activation	No Activation	No Activation
4	614	693	775	614	614
5	No Activation	No Activation	No Activation	No Activation	No Activation
6	991*	477**	825	477**	825
7	296	529	388	296	296
8	674	751	703	674	674
9	211	294	521	211	211
10	1498	1303	Sensor Error	1303	1497
11	No Activation	80*	53	53	53

\*Activated after flaming fire

\*\*Activated during normal cooking

If the false positive is removed from the data set, the theoretical activation occurred on average 74 seconds faster than the element temperature alone, 71 seconds faster than the ionization analog signal alone and 135 seconds faster than the optical density alone as seen in Table 23. As a percentage of the time to flame or experiment length for the hazardous condition the algorithm was 4% faster than element temperature alone, 14% faster than ionization signal alone and 17% faster than optical density alone. A visual representation of the period of algorithm response is presented in Figure 66.

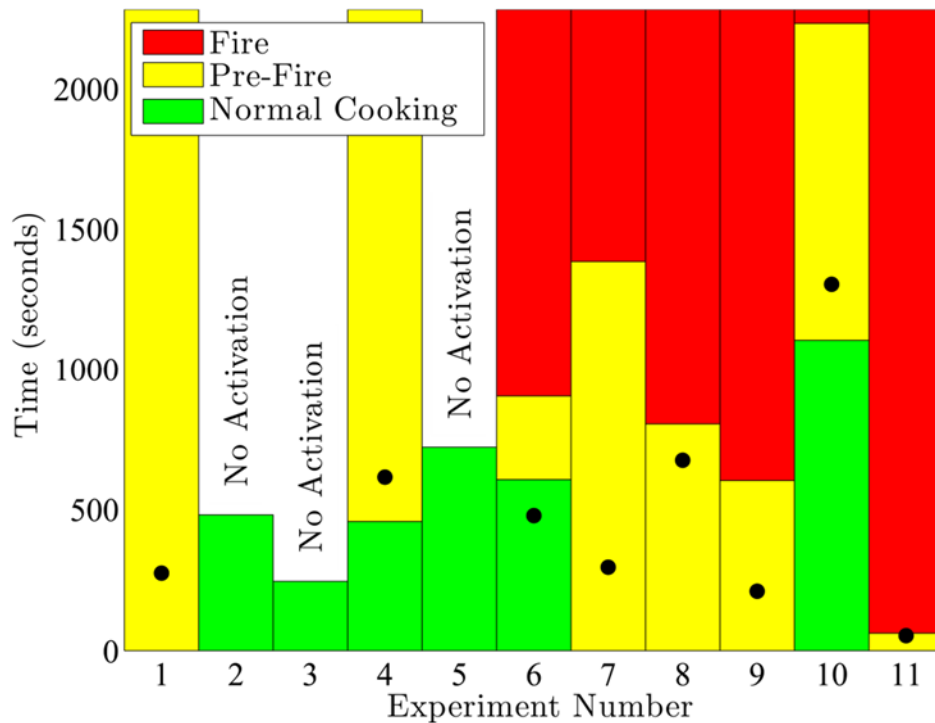


**Figure 66: Multi Sensor Algorithm Performance**

It is possible to create an algorithm which would theoretically identify all 6 impending fires and all 8 hazardous conditions without any false positives. The response of the simplified algorithm takes into consideration the experiment 6 – bacon false positive and removes it by requiring that the element temperature exceed its threshold or the optical density exceeds its threshold, while removing the ionization signal sensor from the logical test. The simplified algorithm logic test graphically shown in Figure 67 is capable of predicting 100% of the impending cooking fires prior to or during the action period identified from range element thermal inertia work by CPSC. In addition it predicts correctly 100% of the hazardous conditions including experiment 11 – pot holder however with a reaction time of only 9 seconds it is likely the thermal inertia effects from the element will still cause a transition to flaming fire. The time of activation is shown in Table 23 compared to the individual sensors and developed algorithm.

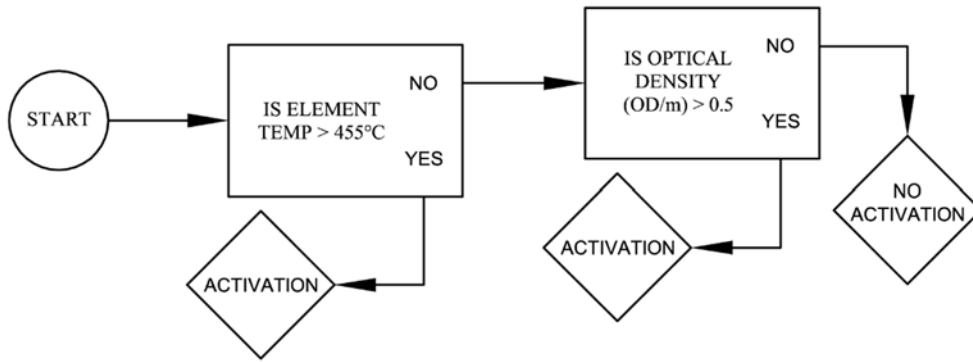


**Figure 67: Simplified Algorithm Logistical Flow Chart**

As compared to the individual sensors and initial algorithm, activation by the simplified algorithm occurred on average 28 seconds faster than the element temperature alone, 33 seconds slower than the ionization analog signal alone 85 seconds faster than the optical density alone and 95 seconds slower than the initial algorithm. As a percentage of the time to flame or experiment length for the hazardous condition, the algorithm was an average of 3% faster than element temperature alone, 4% faster than ionization signal alone and 12% faster than optical density alone but 8% slower than the standard algorithm.

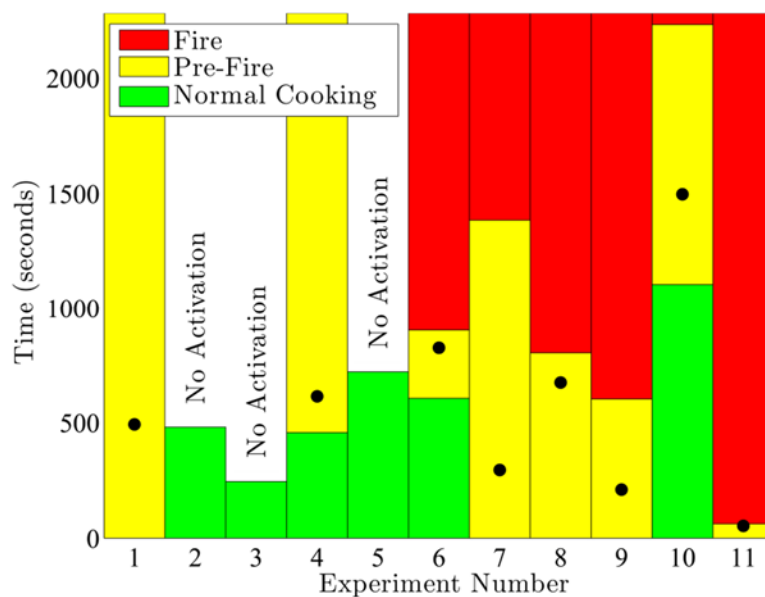


**Figure 68: Simplified Multi Sensor Algorithm Performance**

The combination of optical density and element temperature proves to be the most effective algorithm, however, no more effective than optical density alone. The available reaction time by this combination is increased by an average of 85 seconds over versus the optical density alone. Adjustments in the threshold values may provide more reaction time while maintaining effectiveness but due to the limited size and scope of the data, additional testing is required to validate the use of multiple sensors over a single sensor.



## Chapter 6: Summary

The percentage of structure fires originating in the kitchen continues to grow. Current smoke alarm usage is only relatively effective at identifying an impending cooking fire before it transitions to flaming fire. The high percentage of nuisance activations in kitchen smoke alarms during normal cooking presents a challenge to installing and maintaining smoke alarms in the kitchen. The ability to identify an impending cooking related fire and preventing the transition to flaming fire has the potential to reduce a large percentage of home fires.

Testing conducted by NIST and CPSC has shown pan temperature as a potential indicator of an impending cooking fire. The challenge becomes accurately measuring pan temperature without interrupting the normal cooking process. In an effort to identify additional potential precursor signals to cooking related fires, the eleven cooking experiments were conducted at Underwriters Laboratories (UL). A two-story single family home constructed for other testing had its kitchen outfitted with a functional stove and sensors with the potential to detect impending cooking fires. The experiments recorded optical density, O<sub>2</sub>, CO and CO<sub>2</sub> gas concentrations, temperatures in the environment and of the pan, analog signal from ionization and CO detectors along with monitoring current alarm technologies during both normal cooking and cooking fires.

The data was recorded by UL and transferred to the University of Maryland for subsequent data analysis. It was first separated into normal cooking, pre-fire and fire phases for each experiment through the use of video analysis and thermal inertia data developed by CPSC for oil in metal pans. Then, ranges and average value were analyzed of each phase for all sensors to determine where potential pre-cursor signals may exist. Finally, for those sensors where pre-cursor signals

were detected a threshold was developed and tested against the data set to determine effectiveness. The results indicated element gas temperature, ionization detector signal strength, optical density and carbon monoxide concentration all showed varying levels of potential to detect an impending cooking related fire.

The most prominent precursor signal was the element gas temperature; however it also illustrated potential nuisance alarm scenarios. Similarly ionization signal strength shows potential as a strong precursor signal however it was sensitive to cooking styles where particles are produced such as searing or blackening. Optical density was the most reliable precursor signal however it provided less reaction time than the element gas temperature or ionization signal strength. Although carbon monoxide concentration shows the potential to identify an impending cooking related fire, the reaction time provided may not permit intervention in averting the transition to flaming fire.

In an effort to provide the longest reaction time coupled with the most effective precursor signal, an algorithm can be developed utilizing element gas temperature and optical density values. Utilizing a simple threshold limit for the combined sensors the reaction time can be improved over the individual sensors while still limiting nuisance alarm activations in the data available.

Additional work is required to verify the findings on other cooking styles and to develop a larger data set for analysis of potential cooking fire detection technologies. The data available is only for specific locations in the kitchen constructed and future work should look at collecting data at feasible detector locations.

## Chapter 7: Future Work

### *7.1 Other Cooking Styles*

Due to the limited data set available, additional work should be conducted to validate the identified precursor signals for other cooking styles. Additional normal cooking scenarios such as sautéing, pan frying, stir frying, boiling water and flambé style cooking should be reproduced for evaluation of the identified sensors. The effect of water vapor on the sensors in close proximity to the range is unknown and should be evaluated.

In addition, documented cooking practices should be used to best identify normal cooking practices. For simplicity, the experiments described herein utilized the element temperature set to high and varied the duration of heat exposure to simulate normal cooking. This may be inconsistent with traditional cooking approaches and therefore lead to differing results. This is particularly evident when frying bacon as the bacon grease in the pan began to break down and produce products of combustion between batches of bacon. Had a lower heat setting been utilized, the products may not have been produced in significant quantities to cause the nuisance alarms seen in ionization signal strength or carbon monoxide concentration.

An additional unidentified hazard may exist in cooking foods with a low fat content. Foods such as lean ground beef and vegetables produce significant char layers but do not transition to flaming fire. Tests conducted were stopped after 45 minutes and not permitted to continue heating. Identifying if the potential exists for unattended cooking of foods with low fat and oil content to produce flaming fire should be conducted to quantify the flaming fire hazard.

Reproducible tests of sufficient quantity to identify trends without varying the food cooked or cooking style used can provide the data needed to validate the precursors identified and provide further data to identify effective threshold levels and potential multi sensor algorithms.

Additional cooking scenarios which transition to flaming fires should be conducted such that any trends in time to transition can be identified.

Additionally CPSC research revealed that alcohol sensors indicated higher levels during medium and medium high heat settings, when transition to flaming did not occur (Consumer Product Safety Commission, 1998). The potential exists for this to occur for the identified precursor signals thus low and medium heat settings should be tested with the same food and pan to establish the normal cooking data set.

Lastly an analysis of the cooking fires which occur in the oven versus the cooking fires which occur on the range was not conducted. An understanding of the potential for styles of cooking which utilize an open oven door such as broiling should be tested to verify if transition is possible for foods, and if so, would the developed algorithm be suitable.

## *7.2 Additional Potential Precursor Signals*

The ionization signal strength was a potential precursor signal however additional testing should be conducted to evaluate the effectiveness of higher threshold values on current detection technology. An analog signal from a photoelectric and combination photoelectric and ionization sensor should be tested to potentially identify other current detection technologies which can produce accurate precursor signals. Testing these signals against the current threshold values and

the analog ionization signal may identify multi sensor configurations using advanced algorithm combination photoelectric and ionization alarms.

## References

- Aherns. 2011.** *Smoke Alarms in U.S. Home Fires*. Quincy, MA : NFPA, 2011.
- Ahrens, Marty. 2013.** *Home Structure Fires*. Quincy, MA : National Fire Protection Association, 2013.
- Ansari, Adnan, Guarav, Anchit and Yadav, Vivek. 2010.** *Report of Research on Detection of Kitchen Fire*. Ahmedabad, Gujarat : Underwriters Laboratories Inc., 2010.
- Bukowski, Richard W. 2007.** *Performance of Home Smoke Alarms Analysis of Several Available Technologies in Residential Fire Settings*. Washington : National Institute of Standards and Technology, 2007.
- Cleary, Thomas G. and Chernovsky, Arthur. 2013.** *Smoke Alarm Performance in Kitchen Fires and Nuisance Alarm Scenarios*. Washington, DC : National Institute of Standards and Technology, 2013.
- Consumer Product Safety Commission. 1998.** *Study of Technology for Detecting Pre-Ignition Conditions of Cooking Related Fire Associated with Electric and Gas Ranges: Phase III*. Washington, DC : Consumer Product Safety Commission, 1998.
- Dinaburg, Joshua and Guttok, Ph.D, P.E., Daniel T. 2011.** *Home Cooking Fire Mitigation: Technology Assessment*. Quincy, MA : The Fire Protection Research Foundation, 2011.
- Federal Emergency Management Agency. 2013.** *Cooking Fires in Residential Buildings*. Emmitsburg, MD : Federal Emergency Management Agency, 2013.
- Feng, Jewell T. and Milke, James A. 2012.** *Analysis of the Response of Smoke Detectors to Smoldering Fires and Nuisance Sources*. College Park, MD : University of Maryland, 2012.
- Greene, Michael A. and Andres, Craig. 2009.** *2004-2005 National Sample Survey of Unreported Residential Fires*. s.l. : U.S. Consumer Product Safety Commission, 2009.
- Hagen, Bjarne Christian. 1994.** *Evaluation of Gaseous Signatures in Large-Scale Test*. College Park, MD : University of Maryland, 1994.
- Johnsson, Erik L. 1998.** *Study of Technology for Detecting Pre-Ignition Conditions of Cooking-Related Fires Associated with Electric and Gas Ranges and Cooktop, Final Report*. Gaithersburg, MD : National Institute of Standards and Technology, 1998.
- . 1995.** *Study of Technology for Detecting Pre-Ignition Conditions of Cooking-Related Fires Associated with Electric and Gas Ranges and Cooktops, Phase I Report*. Gaithersburg, MD : National Institute of Standards and Technology, 1995.
- Levesque, Paula. 2013.** *Trends and Patterns of U.S. Fire Losses in 2011*. Quincy, MA : National Fire Protection Association , 2013.
- Smith, Charles L. 1994.** *Smoke Detector Operability Survey Report on Findings*. s.l. : Consumer Product Safety Commission, 1994.
- Universal Security Instruments, Inc. 2013.** *The New IoPhic Universal Sensing Technology from Smoke Alarms.com*. [Online] 2013. [Cited: September 3, 2013.] <http://smokealarms.com/iophic.htm>.